Available online at www.sciencedirect.com
ScienceDirect
Bioorganic & Medicinal Chemistry 16 (2008) 1927–1947
Bioorganic & Medicinal Chemistry

Anti-*Plasmodium* activity of tetrazolium salts

Xilin Cui,[a] Jason Z. Vlahakis,[a] Ian E. Crandall[b,*] and Walter A. Szarek[a,*]

[a]*Department of Chemistry, Queen's University, Kingston, ON, Canada K7L 3N6*
[b]*Department of Laboratory Medicine and Pathobiology, University of Toronto, Toronto, ON, Canada M5S 1A8*

Received 25 May 2007; revised 23 October 2007; accepted 1 November 2007
Available online 5 November 2007

Abstract—We have previously reported that sulfated cyclodextrins inhibit the invasion of *Plasmodium* merozoites by interacting with receptors present on the surface of erythrocytes. The observation that tetrazolium salts formed stable complexes with the inhibitory sulfated cyclodextrins suggested that tetrazolium salts might have anti-*Plasmodium* activity as well. Evaluation of commercially available tetrazolium salts indicated that some were active in the low nanomolar range and showed specificity in their inhibition of *Plasmodium*. Synthesis of a further 54 structures allowed us to determine that activity results from an aromatic component attached to the tetrazolium carbon atom (R^1) and its size is not critical to the activity of the compound. Nitro modifications of active compounds are poorly tolerated, however, the presence of halogen atoms on aromatic groups attached to the nitrogen atoms of the tetrazolium ring (R^2 and R^3) has little effect on activity. Methoxy groups are tolerated on R^2 and R^3 components; however, they are disruptive on the R^1 component. The overall results suggest that the R^1 component is interacting with a specific hydrophobic environment and the R^2 and R^3 components are less constrained. The activity of these compounds in several human and mouse *Plasmodium* cultures suggests that the compounds interact with a component of the parasite that is both essential and conserved.

1. Introduction

The number of people who are at risk of acquiring malaria is not known precisely, however, some estimates are as high as 3.2 billion people with up to 500 million clinical cases per year.[1] Further, malaria contributes to the deaths of 1–3 million people per year,[2] most of them young children. The continued spread of resistance to antimalarials such as chloroquine[3] has produced a desperate need for safe and inexpensive antimalarial agents having novel mechanisms of action. Our previous work[4] demonstrated that small sulfonated compounds inhibited the entry of merozoites of *Plasmodium falciparum* into human erythrocytes, and were able also to suppress the replication of *Plasmodium berghei* in mice. The interactions between a merozoite and an erythrocyte that are responsible for the invasion process are complex;[5] however, individual *Plasmodium* species are frequently limited to a particular host, or even a particular stage of development of an erythrocyte, by the specificity of the ligand/receptor interactions involved in erythrocyte invasion.[6] The invasion process is rapid, typically 15–30 s,[7] and is divided frequently into three stages: (1) the initial attachment of the merozoite to the erythrocyte followed by reorientation of the merozoite such that its apical end is proximal to the erythrocyte; (2) the secretion and anchoring of proteins required to form a 'tight junction' with the erythrocyte membrane; and (3) physical insertion.[8] While the receptors required for tight-junction formation are reasonably well characterized[9] the identities of the molecules responsible for the initial contact events are unclear.

Treatment of erythrocytes with sulfated cyclodextrins leads to an increase in surface staining with cationic dyes,[10] an observation that is consistent with the compounds' interaction with an erythrocyte surface component. While the inhibitory activity of these compounds may result entirely from non-specific effects, such as repulsive negative surface charges,[11] alterations in the conformations of surface receptors,[12] or changes in the multimerization state of the receptor proteins,[13] our previous work[10] suggested that a specific mechanism was responsible since sulfated cyclodextrins could be displaced effectively from erythrocytes by stilbene disulfonates. Stilbene disulfonates, such as SITS (4-acetamido-4′-isothiocyanato-2,2′-stilbenedisulfonic acid

Keywords: *Plasmodium falciparum*; Tetrazolium salts; Malaria.
* Corresponding authors. Tel.: +1 416 581 7704; fax: +1 416 978 8765 (I.E.C.); tel.: +1 613 533 2643; fax: +1 613 533 6532 (W.A.S.); e-mail addresses: ian.crandall@utoronto.ca; walter.szarek@chem.queensu.ca

0968-0896/$ - see front matter © 2007 Elsevier Ltd. All rights reserved.
doi:10.1016/j.bmc.2007.11.005

disodium salt) and DIDS (4,4′-diisothiocyanatostilbene-2,2′-disulfonic acid disodium salt), are highly specific inhibitors of the erythrocyte anion-exchange protein AE1, also known as band 3.[14] An opportunity to test the hypothesis that sulfated cyclodextrins or stilbene disulfonates share a surface topology and charge distribution with a merozoite ligand arose when we observed that commercially available tetrazolium salts, which are components of our viability assays, could not be reduced in the presence of sulfated cyclodextrins or stilbene disulfonates. We reasoned that, if a merozoite ligand were composed of an anionic glycan, then tetrazolium salts might be able to prevent merozoite attachment and invasion. Interestingly, it has been reported[15] that mono- and bis-thiazolium salts have potent antimalarial activity; these compounds target the plasmodial phospholipid metabolism. In the present work, the anti-*Plasmodium* activities of eight commercially available tetrazolium salts were evaluated and it was observed that several compounds inhibited *P. falciparum* cultures in the nanomolar range. To explore further the potential relationship between structure and activity an additional fifty-four tetrazolium salts were synthesized. Our findings suggest that tetrazolium compounds may form the basis for a novel class of antimalarials.

2. Synthesis

The **QT** series of tetrazolium compounds (see Fig. 1, for generic structure) were synthesized according to the general synthetic route shown in Scheme 1. In the first step, a substituted alkyl- or aryl- aldehyde was condensed with a substituted phenylhydrazine in acidic MeOH to form the hydrazone derivative. Concurrently, a substituted aryldiazonium salt was freshly prepared from a substituted aromatic amine by treatment with concentrated hydrochloric acid and sodium nitrite.[16,17] The formazan was then prepared by an azo coupling reaction of the hydrazone derivative with the diazonium salt in pyridine. Oxidation of the formazan to the tetrazolium salt was then accomplished using freshly prepared *tert*-butyl hypochlorite[18] in chloroform. Using this four-step methodology, a wide variety of functionalized tetrazolium salts were synthesized using three commercially available starting materials (alkyl- or aryl- aldehydes, arylhydrazines, and arylamines). The wide diversity of available starting materials and control over the position of substituents on the tetrazolium ring allowed us to explore systematically structure–activity relationships of almost sixty compounds (see Table 1) with a view of finding effective antimalarial drug candidates. The R^1 substituent (originating from the aldehyde) is attached at a unique position on the tetrazolium ring, however, because of charge delocalization in the tetrazolium ring the R^2 and R^3 positions are interchangeable (see Fig. 1).

3. Biological evaluation

When sulfated cyclodextrins were being evaluated for their ability to inhibit the entry of *P. falciparum* merozoites into erythrocytes it was observed[10] that at higher concentrations some of the sulfated compounds also inhibited the LDH assay employed in the parasite viability studies.[19] Further investigation indicated that sulfated cyclodextrins had no effect on the activity of the *P. falciparum* or mammalian lactate dehydrogenase enzymes or the diaphorase enzyme used in the assay[19] (data not shown), however, in the presence of sulfated cyclodextrins, nitrotetrazolium blue chloride (NBT) could not be reduced to the corresponding formazan dye by reducing agents such as glutathione. Non-sulfated cyclodextrins had no effect on the reduction of NBT, a result suggesting that the negatively charged sulfate groups formed a high-affinity complex with the electron-deficient tetrazolium ring thereby stabilizing it against reduction to the uncharged formazan. We have hypothesized[10] that sulfated cyclodextrins might share charge and topographical features with stilbene disulfonates such as SITS (4-acetamido-4′-isothiocyanato-2,2′-stilbenedisulfonic acid disodium salt) and DIDS (4,4′-diisothiocyanatostilbene-2,2′-disulfonic acid disodium salt), an aspect which might allow sulfated cyclodextrins to compete with these compounds for the ''DIDS site'' in AE1.[20] DIDS and SITS also inhibited the reduction of NBT by glutathione. The observation that a tetrazolium salt interacted with stilbene disulfonates or sulfated cyclodextrins suggested that if a merozoite ligand shared common structural features with these agents then tetrazolium salts should have anti-*P. falciparum* properties. To test this hypothesis, the effects of eight commercially available tetrazolium salts on the viability of *P. falciparum* cultures were evaluated (see Table 1) and the potency was compared to the toxicity observed in a mammalian cell line, namely Chinese Hamster Ovary (CHO) cells. Some tetrazolium salts, such as thiazoyl blue tetrazolium bromide (MTT), nitrotetrazolium blue chloride (NBT), and tetranitroblue tetrazolium chloride, produced oxidative erythrocyte lysis; however, others, such as tetrazolium red and tetrazolium violet, were found to inhibit parasite viability in the low micromolar range (see Table 1 and Fig. 4). Microscopic examination of the treated wells revealed images that were consistent with merozoite invasion being inhibited; however, other toxic effects could be possible. Compounds such as tetrazolium red and tetrazolium violet were found to be tolerated relatively well by mammalian cells (see Table 1 and Fig. 4), a result that suggested that these compounds might inhibit a process that was specific to the viability of *P. falciparum* cultures. As regards the bioavailability of the tetrazolium salts, it is known that such compounds are able to cross membranes and indeed this ability is the basis of the MTT (3-[4,5-dimethylthiazol-2-yl]-2,5-diphenyltetrazolium bromide) assay.[21]

To determine if tetrazolium salts inhibited a process that was specific to a particular tight-junction receptor the effects of tetrazolium violet on other laboratory *P. falciparum* isolates and two murine malarias were evaluated. Tetrazolium violet was found to have similar potency in the laboratory lines ItG, 3D7, and FCR3 (Fig. 5), and similar results were obtained with the murine malarias, *P. berghei* and *Plasmodium chabaudi chabaudi*. *P. falciparum* lines that were grown in erythrocyte cultures, that had been treated either with neuraminidase or tryp-

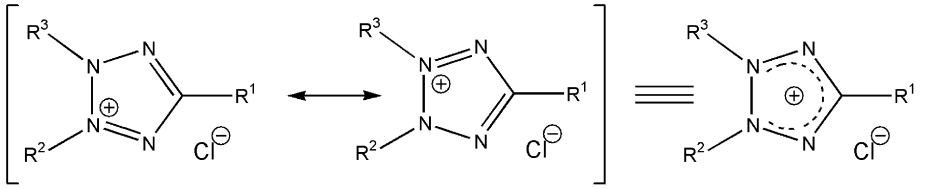

Figure 1. Generic structure for tetrazolium salts.

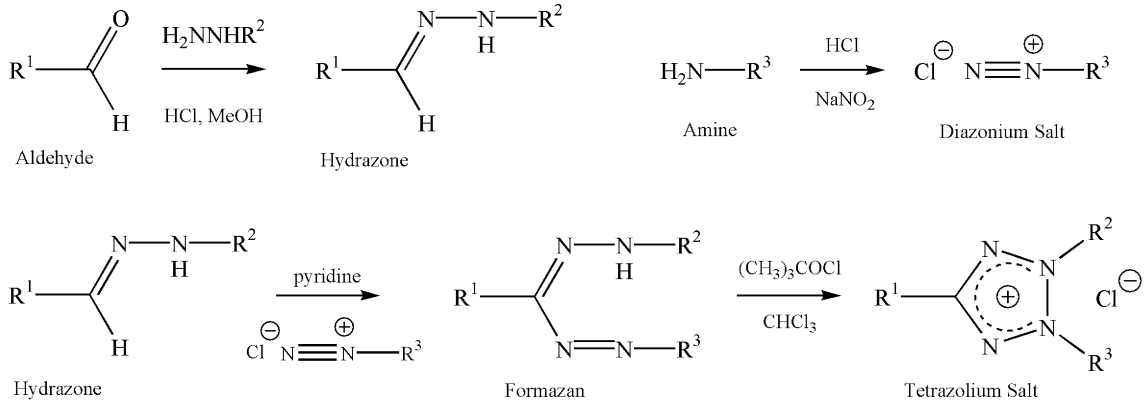

Scheme 1. General synthetic strategy for the generation of tetrazolium salts.

sin,[22,9] were also found to yield similar IC_{50} values, an observation suggesting that the process being targeted was common to many species and lines of *Plasmodium* and was not specific to a particular tight-junction receptor.

Our analysis of the results obtained with the commercially available tetrazolium salts suggested that further variation of the R^1, R^2, and/or R^3 moieties might produce agents with even more desirable anti-*Plasmodium* properties. Thus, fifty-four compounds (**QT1–QT54**) were synthesized and evaluated in both *P. falciparum* and CHO cell cultures (Table 1). A wide range of activities and specificities for *P. falciparum* cultures was observed. Microscopic examination of the inhibited assay wells confirmed that the active agents produced large numbers of extracellular merozoites, a feature consistent with the hypothesis that inhibition of merozoite entry is the primary mechanism of action of these compounds (data not shown).

Complex anionic glycans have been shown previously to inhibit *P. falciparum* cultures,[4,23] a result which was attributed to their binding to the surface of an erythrocyte and creating a surface charge that repelled merozoites.[11] The ability of sulfated cyclodextrins to inhibit *P. falciparum* cultures might be explained by a similar mechanism, however, the observation that NBT could not be reduced to the corresponding formazan in the presence of these inhibitors permitted a testing of the hypothesis that sulfated cyclodextrins mimicked a feature present in a potential merozoite ligand. The interaction of NBT with anions presumably results from the electron-deficient ring of a tetrazolium salt being attracted by the electron-rich sulfate groups of sulfated cyclodextrins,[24] and the R groups surrounding the tetrazolium ring would either inhibit or enhance this process. The envisioned complex would appear to be unusually stable since the results of the assays, involving varying amounts of sulfated cyclodextrins, when plotted (Fig. 2) produce a series of lines having similar slopes instead of a series of lines having different slopes that intersect at the origin, a result suggesting that sulfated cyclodextrins are effectively removing a stoichiometric amount of NBT from the reaction well. The observation that NBT also interacts with the stilbene disulfonates DIDS and SITS (Fig. 3) compounds that bind with a high affinity and specificity to a defined site in the erythrocyte anion transport protein,[20] is in agreement with previous reports[25,26] that AE1 participates in merozoite invasion and suggests that tetrazolium salts interact with either MSP1 or MSP9. While Kariuki et al.[26] favor the hypothesis that the MSP1/MSP9 complex is involved in tight-junction formation, our data support the hypothesis that the DIDS site in AE1 is the receptor used in the initial recognition/tethering interaction of the merozoite. The ability of tetrazolium salts and sulfated cyclodextrins to reduce the viability of multiple lines and species of *Plasmodium* is consistent with the highly conserved nature of the DIDS site.[27] Furthermore, the ability of similar concentrations of tetrazolium violet to inhibit the entry of multiple *P. falciparum* lines into human erythrocytes and two species of murine *Plasmodium* into murine erythrocytes (Fig. 5) is consistent with the targeting of a conserved ligand structure.

Variations in the structure of tetrazolium salts can have several important effects in culture assays. For example, reduction of the tetrazolium ring to the corresponding formazan is dependent in part on the presence of electron-withdrawing groups in the surrounding rings, a fea-

Table 1. Activities of tetrazolium salts in CHO and *P. falciparum* cultures[a]

Compound	Structure	IC_{50} (μM) *P. falciparum*	IC_{50} (μM) CHO cells	IC_{50} CHO/IC_{50} *P. falciparum*
Tetrazolium red	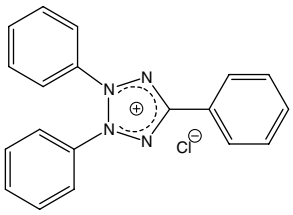	0.3 ± 0.2	71 ± 15	236.7
Tetrazolium violet	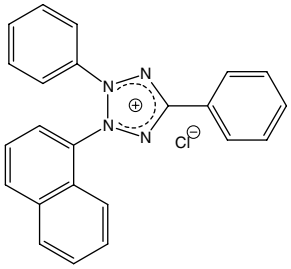	0.15 ± 0.05	15 ± 3	100.0
Iodonitrotetrazolium chloride	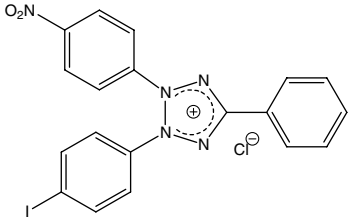	81 ± 16	49 ± 12	0.6
Thiazoyl blue tetrazolium bromide (MTT)	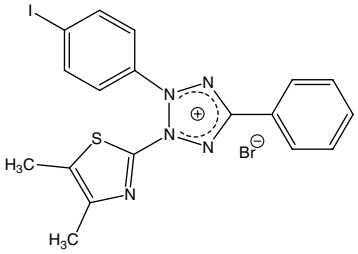	[b]	[c]	—
Neotetrazolium chloride	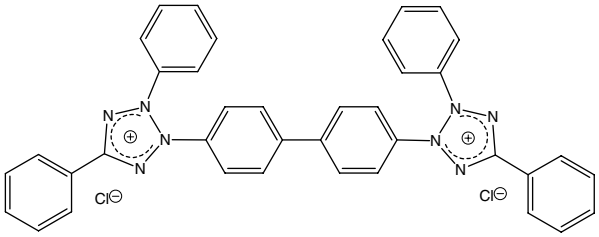	0.35 ± 0.08	11 ± 3	31.4
Tetrazolium blue chloride	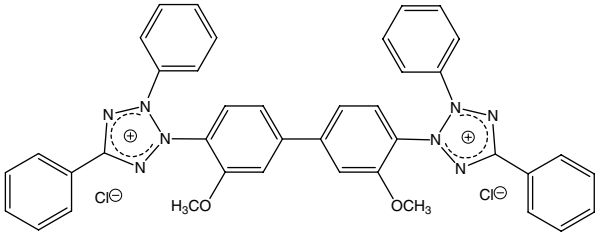	3.8 ± 0.3	>100	—

Table 1 (*continued*)

Compound	Structure	IC_{50} (μM) *P. falciparum*	IC_{50} (μM) CHO cells	IC_{50} CHO/IC_{50} *P. falciparum*
Nitrotetrazolium blue chloride	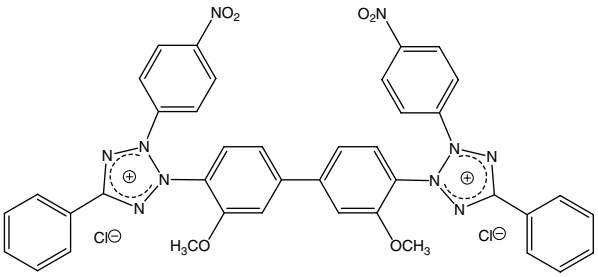	[b]	[c]	—
Tetranitroblue tetrazolium chloride	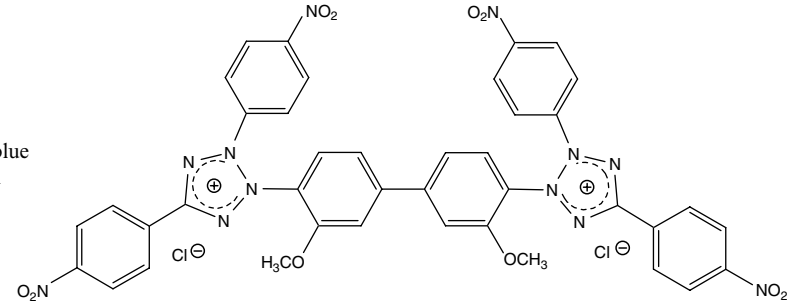	[b]	1.3 ± 0.4	—
QT1	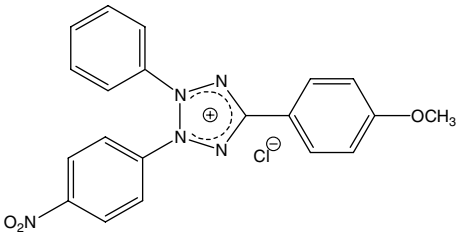	3.7 ± 0.6	6 ± 3	1.6
QT2	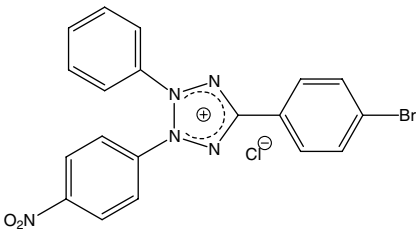	10.0 ± 0.9	7 ± 1	0.7
QT3	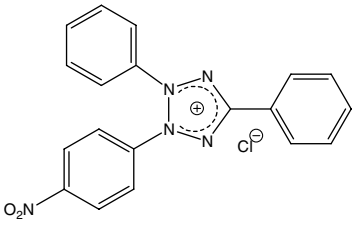	4.5 ± 0.6	12 ± 1	2.7
QT4	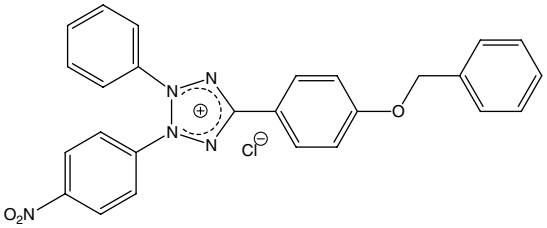	9 ± 3	4.4 ± 0.8	0.5

(*continued on next page*)

Table 1 (*continued*)

Compound	Structure	IC_{50} (μM) *P. falciparum*	IC_{50} (μM) CHO cells	IC_{50} CHO/IC_{50} *P. falciparum*
QT5	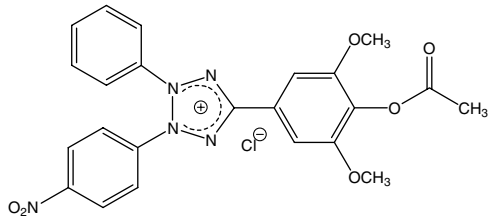	7.3 ± 0.9	19 ± 4	2.6
QT6	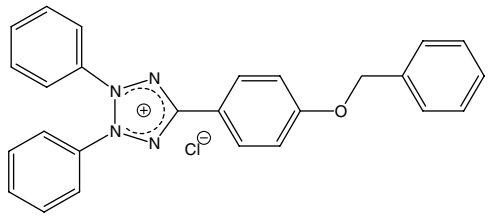	0.103 ± 0.008	4.2 ± 0.9	40.8
QT7	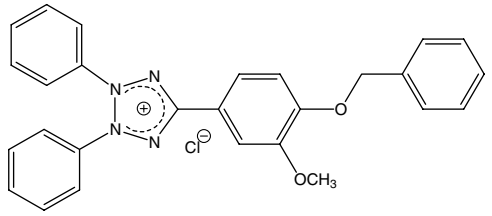	0.26 ± 0.03	4.7 ± 0.4	18.1
QT8	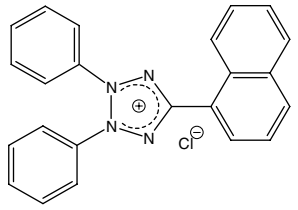	0.35 ± 0.03	2.4 ± 0.5	6.9
QT9	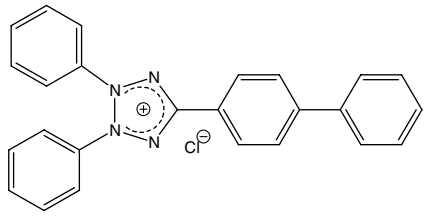	0.23 ± 0.02	7 ± 1	30.4
QT10	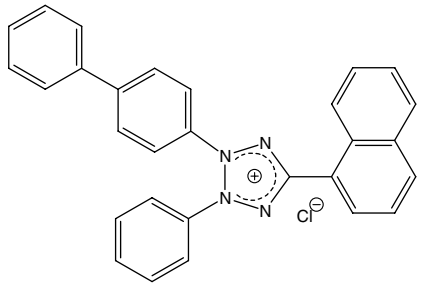	2.9 ± 0.2	9 ± 1	3.1
QT11	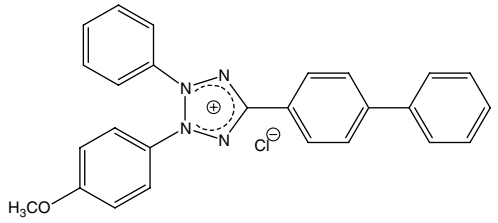	0.43 ± 0.04	19 ± 4	44.2

Table 1 (*continued*)

Compound	Structure	IC_{50} (μM) *P. falciparum*	IC_{50} (μM) CHO cells	IC_{50} CHO/IC_{50} *P. falciparum*
QT12	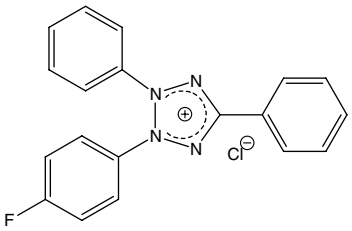	0.93 ± 0.06	39 ± 6	41.9
QT13	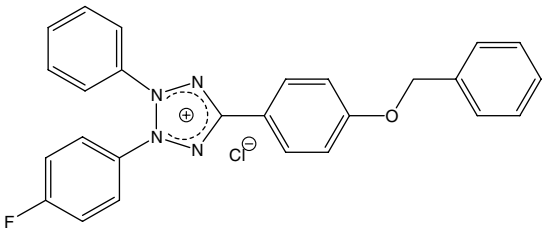	0.47 ± 0.01	16 ± 2	34.0
QT14	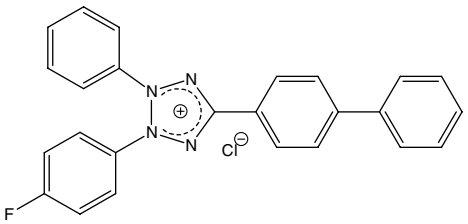	0.81 ± 0.04	4.1 ± 0.6	5.1
QT15	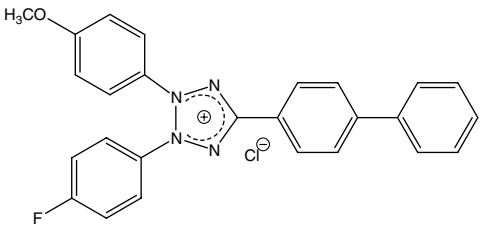	1.7 ± 0.2	19 ± 2	11.2
QT16	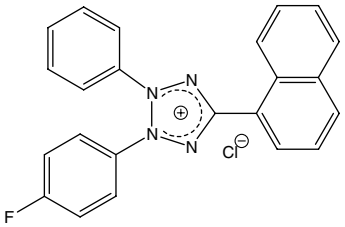	0.83 ± 0.09	32 ± 3	38.6
QT17	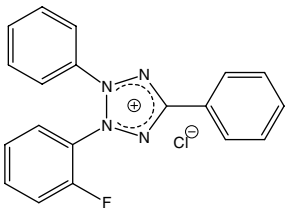	0.39 ± 0.09	44 ± 4	112.8
QT18	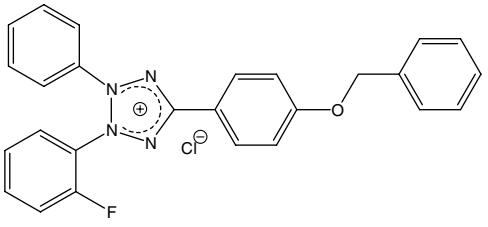	0.14 ± 0.02	8 ± 1	57.1

(*continued on next page*)

Table 1 (*continued*)

Compound	Structure	IC_{50} (μM) *P. falciparum*	IC_{50} (μM) CHO cells	IC_{50} CHO/IC_{50} *P. falciparum*
QT19	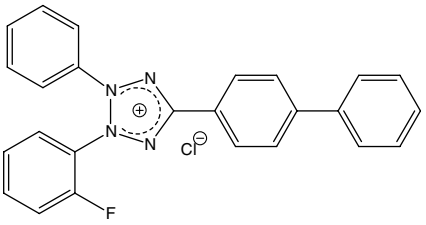	0.36 ± 0.08	8 ± 1	22.2
QT20	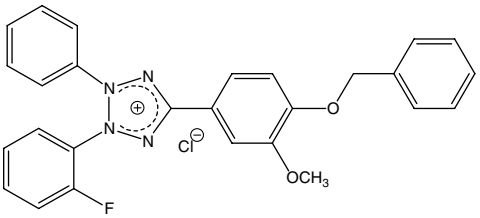	2.2 ± 0.3	2.7 ± 0.4	1.2
QT21	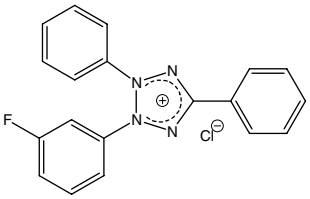	2.2 ± 0.2	36 ± 3	16.4
QT22	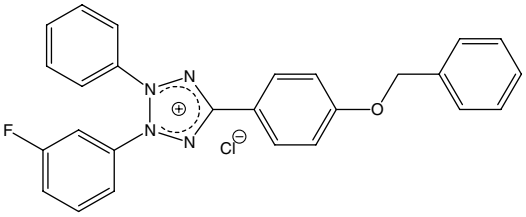	0.42 ± 0.03	4.3 ± 0.5	10.2
QT23	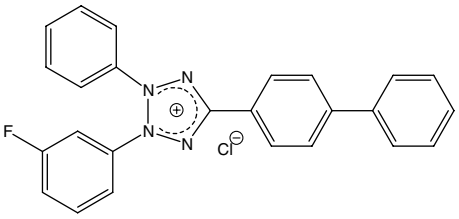	0.26 ± 0.03	4.9 ± 0.5	18.8
QT24	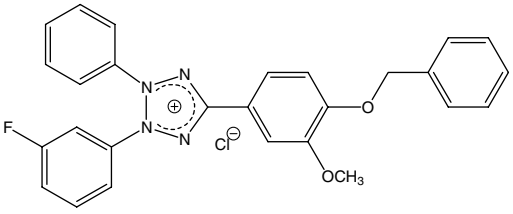	3.2 ± 0.5	6.5 ± 0.7	2.0
QT25	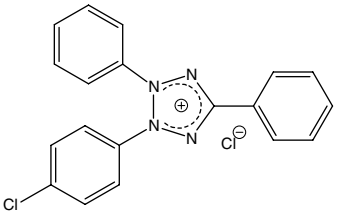	0.63 ± 0.01	39 ± 3	61.9

Table 1 (*continued*)

Compound	Structure	IC_{50} (μM) *P. falciparum*	IC_{50} (μM) CHO cells	IC_{50} CHO/IC_{50} *P. falciparum*
QT26	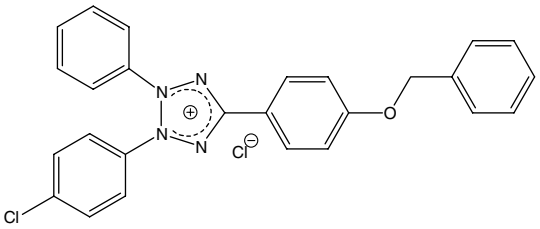	1.14 ± 0.05	4.6 ± 0.8	4.0
QT27	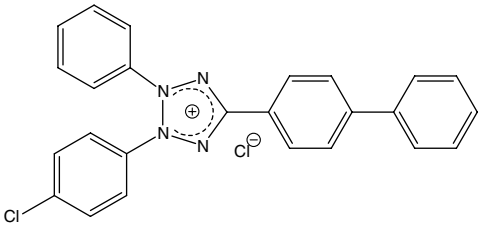	0.41 ± 0.09	16 ± 5	39.0
QT28	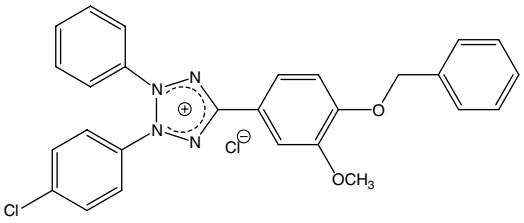	3.8 ± 0.2	32 ± 8	8.4
QT29	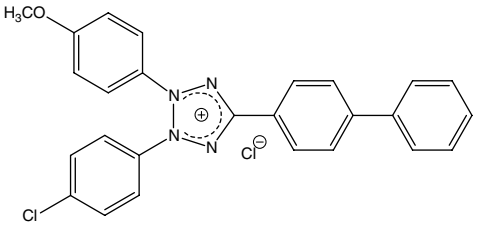	0.40 ± 0.01	12 ± 2	30.0
QT30	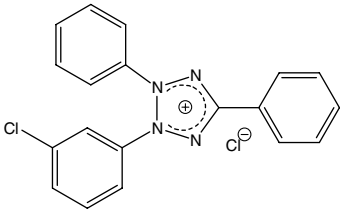	0.84 ± 0.05	6.3 ± 0.6	7.5
QT31	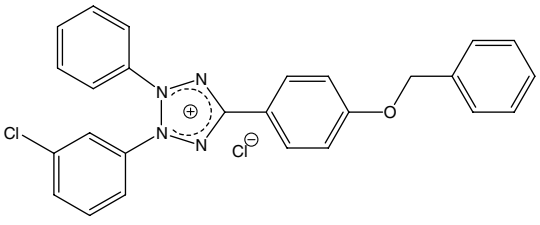	0.08 ± 0.01	9 ± 4	112.5
QT32	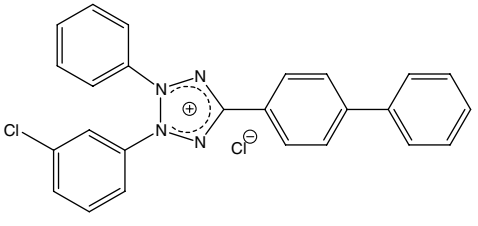	0.115 ± 0.008	10 ± 2	87.0

(*continued on next page*)

Table 1 (*continued*)

Compound	Structure	IC_{50} (μM) *P. falciparum*	IC_{50} (μM) CHO cells	IC_{50} CHO/IC_{50} *P. falciparum*
QT33	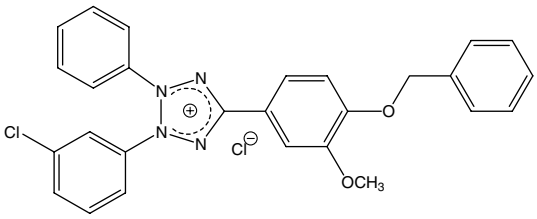	0.69 ± 0.07	8 ± 1	11.6
QT34	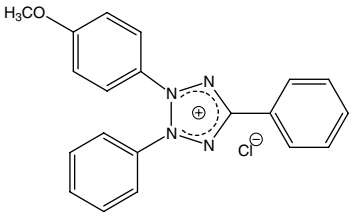	0.80 ± 0.08	6.5 ± 0.9	8.1
QT35	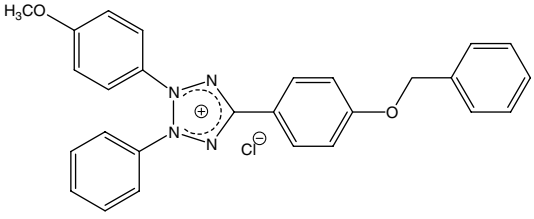	0.32 ± 0.03	9 ± 2	28.1
QT36	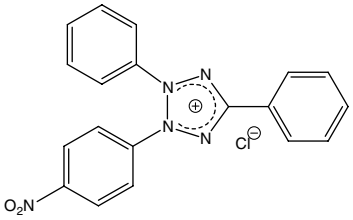	9.1 ± 0.5	16.2 ± 0.9	1.8
QT37	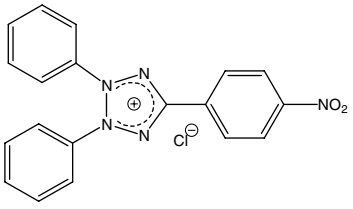	14 ± 2	31 ± 2	2.2
QT38	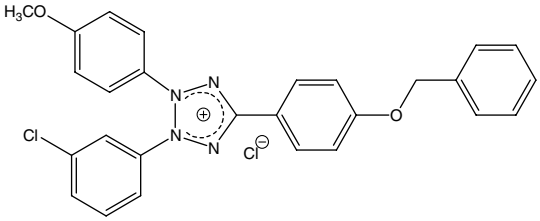	0.29 ± 0.01	16 ± 4	55.2
QT39	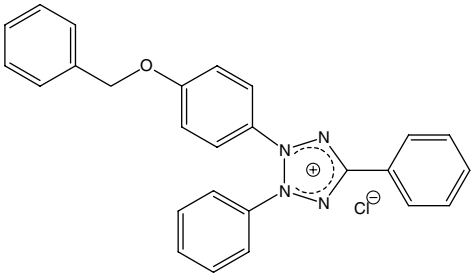	0.200 ± 0.009	37 ± 4	185.0

Table 1 (*continued*)

Compound	Structure	IC_{50} (μM) *P. falciparum*	IC_{50} (μM) CHO cells	IC_{50} CHO/IC_{50} *P. falciparum*
QT40	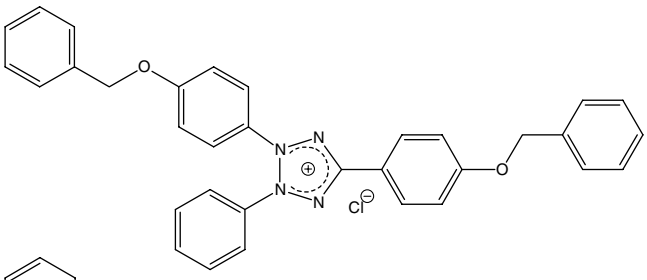	0.23 ± 0.01	0.96 ± 0.09	4.2
QT41	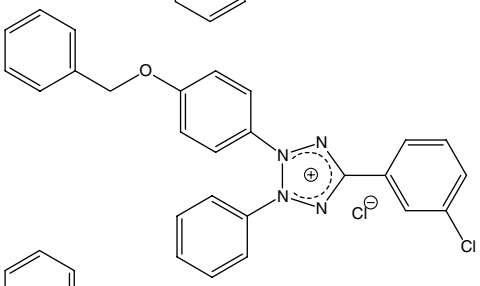	0.41 ± 0.02	38 ± 4	92.7
QT42	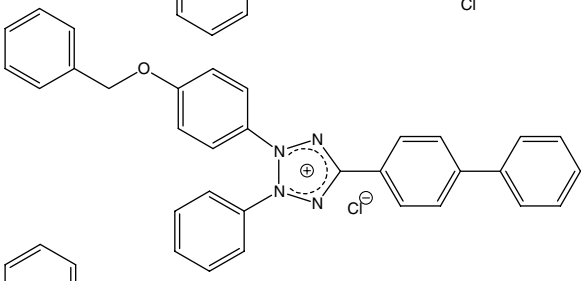	0.261 ± 0.008	1.7 ± 0.3	6.5
QT43	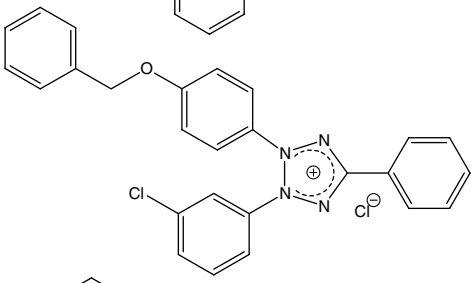	0.10 ± 0.02	14 ± 1	140.0
QT44	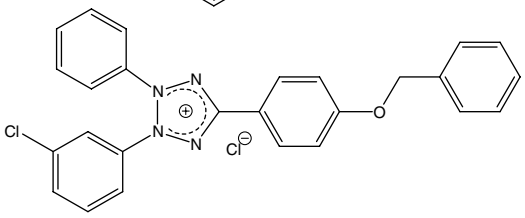	0.33 ± 0.03	7 ± 1	21.2
QT45	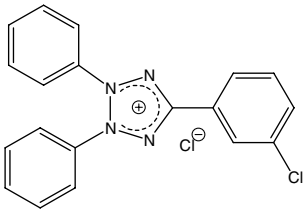	0.46 ± 0.02	43 ± 5	93.5
QT46	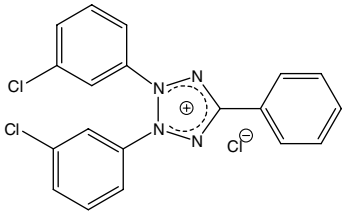	0.5 ± 0.1	36 ± 5	72.0

(*continued on next page*)

Table 1 (*continued*)

Compound	Structure	IC_{50} (μM) *P. falciparum*	IC_{50} (μM) CHO cells	IC_{50} CHO/IC_{50} *P. falciparum*
QT47	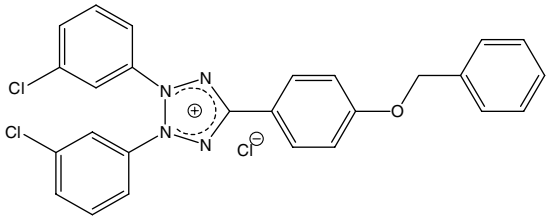	1.3 ± 0.1	21 ± 4	16.2
QT48	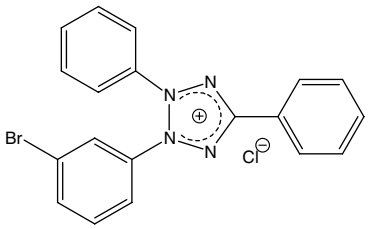	0.6 ± 0.1	6.4 ± 0.5	10.7
QT49	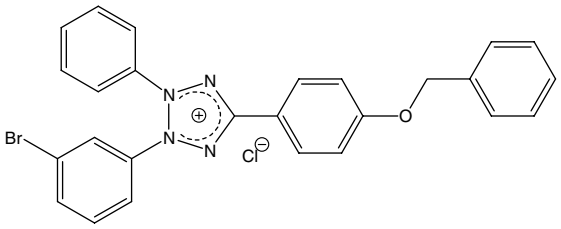	0.4 ± 0.1	8.1 ± 0.6	20.3
QT50	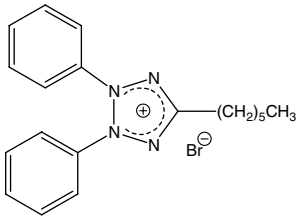	3.4 ± 0.4	21 ± 3	6.2
QT51	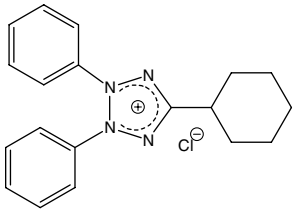	6.2 ± 0.5	25 ± 1	4.0
QT52	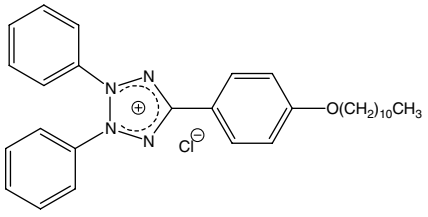	4 ± 1	0.40 ± 0.03	0.1
QT53	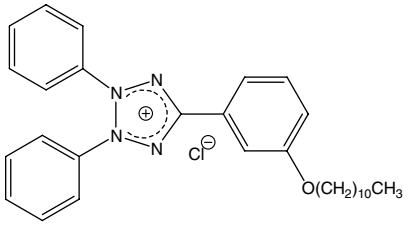	2.5 ± 0.5	5.0 ± 0.7	2.0

Table 1 (*continued*)

Compound	Structure	IC_{50} (μM) *P. falciparum*	IC_{50} (μM) CHO cells	IC_{50} CHO/IC_{50} *P. falciparum*
QT54	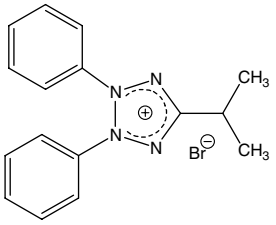	102 ± 19	377 ± 27	3.7

[a] Each IC_{50} value represents the mean of four determinations with standard error indicated. The 'ratio of activities' given in the fifth column represents the IC_{50} value determined for CHO cells divided by the IC_{50} value determined for *P. falciparum* cultures. Values greater than unity indicate that the compound has greater potency in *P. falciparum* cultures. The strain line used was ItG.
[b] Oxidizes erythrocytes.
[c] Not determined.

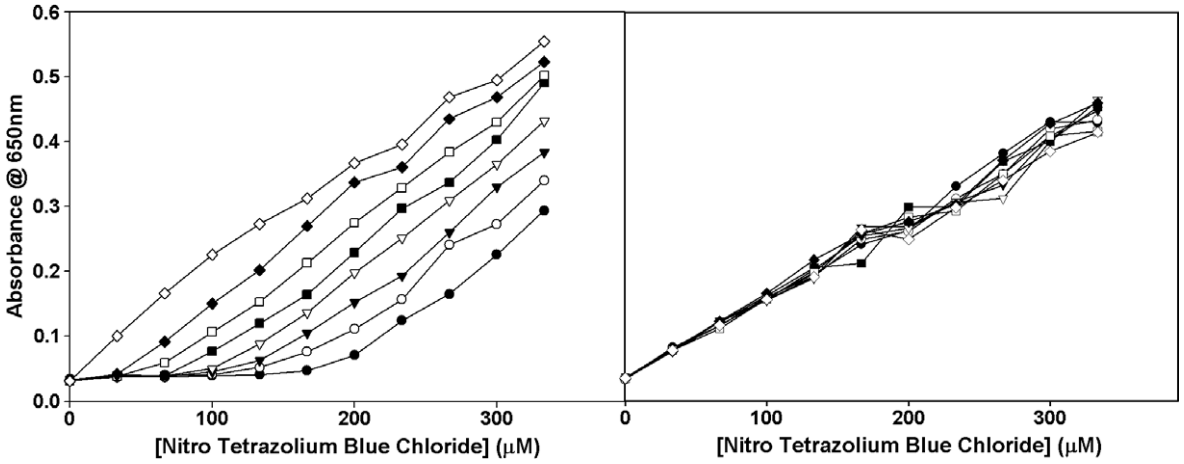

Figure 2. Effect of β-cyclodextrins on nitrotetrazolium blue chloride (NBT). The ability of β-cyclodextrins to inhibit the reduction of NBT was determined. Varying concentrations of NBT (indicated on *x*-axis) and β-cyclodextrin were incubated together prior to the addition of glutathione. After 10 min the absorbance at 650 nm of the individual wells was determined. The left panel indicates the results obtained with a β-cyclodextrin having an average of 1 sulfate group per glucose residue; the right panel represents β-cyclodextrin having no sulfate groups. Symbols indicate final β-cyclodextrin concentrations: ◇ 0 μM; ♦ 24 μM; □ 48 μM; ■ 71 μM; ▽ 95 μM; ▼ 119 μM; ○ 142 μM; and ● 167 μM.

ture which determines how well these compounds function as oxidants. The presence of nitro groups, as in iodonitrotetrazolium chloride, nitrotetrazolium blue chloride, tetranitroblue tetrazolium chloride, and **QT1–QT5**, appears to make these compounds generally toxic and therefore they showed little specificity for *Plasmodium*. Conversely, the absence of nitro groups, as in tetrazolium red, tetrazolium violet, neotetrazolium chloride, tetrazolium blue chloride, and the majority of the **QT** compounds, appears to allow a selectivity of activity against *Plasmodium*. The best example of this general trend can be seen by comparing the potency of tetrazolium red to that of **QT36** and **QT37**. This finding is consistent with our hypothesis that it is the tetrazolium form of the compounds that are active because they complex with components of the parasite that are essential for its viability. Formazans lack the electron deficiency that we consider to be essential for activity and therefore reduction of the tetrazolium rings may render the compounds inactive.

It is noteworthy that compounds **QT12**, **QT17**, **QT21**, **QT25**, **QT30**, **QT45**, **QT46**, and **QT48** which contain fluoro, chloro, or bromo groups at *ortho*, *meta*, or *para* positions, all display similar potency and reasonable selectivity when compared to their parent compound, tetrazolium red. Multivalency does not seem to be relevant for activity as evidenced by a comparison of the potency of monovalent tetrazolium red and divalent neotetrazolium chloride.

The effect of changing the R^1 components of the tetrazolium compounds was examined by different approaches. Tetrazolium red had excellent anti-*Plasmodium* activity, however, increasing the size of this group, as in **QT6, QT8,** and **QT9**, does not greatly affect potency. However, when aliphatic or alicyclic groups are added at the R^1 position, as in **QT50–54,** both potency and selectivity are compromised. The incorporation of halogen atoms (F or Cl) to compounds having larger R^1 groups, for example, a biphenyl group, is also permissible since modifying **QT9** to produce **QT14**, **QT19**, **QT23**, **QT27**, and **QT32** gives compounds that are still both active and selective. Similarly, incorporation of halogen into **QT6** affords compounds **QT13**, **QT18**, **QT22**, **QT26**, **QT31**, **QT44**, **QT47**, and **QT49** which have desir-

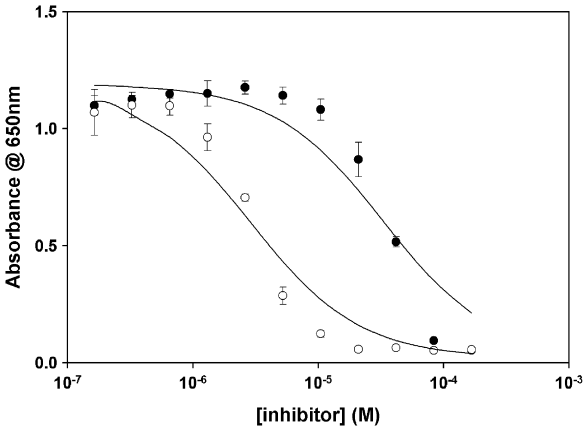

Figure 3. Effect of DIDS and SITS on nitrotetrazolium blue chloride (NBT). NBT was added to microwells containing a serial dilution series of either DIDS (●) or SITS (○) and allowed to incubate for 10 min. To determine the amount of unbound NBT present, glutathione in Tris buffer was added to every well and after 10 min the absorbance at 650 nm was determined. Data points are the mean of four determinations with the standard error indicated by error bars. The IC_{50} values of individual compounds were determined using a non-linear regression analysis of the dose–response curve and IC_{50} values of 31 ± 2 μM and 2.7 ± 0.1 μM were determined for DIDS and SITS, respectively.

able potency and selectivity. The addition of methoxy groups to the R^2 and R^3groups is also well tolerated as regards useful effects, for example, **QT27** versus **QT29**, tetrazolium red versus **QT34**, and **QT9** versus **QT11**; however, the addition of a methoxy group to an R^1 group can be disruptive, for example, **QT18** versus **QT20**, **QT22** versus **QT24**, and **QT31** versus **QT33**.

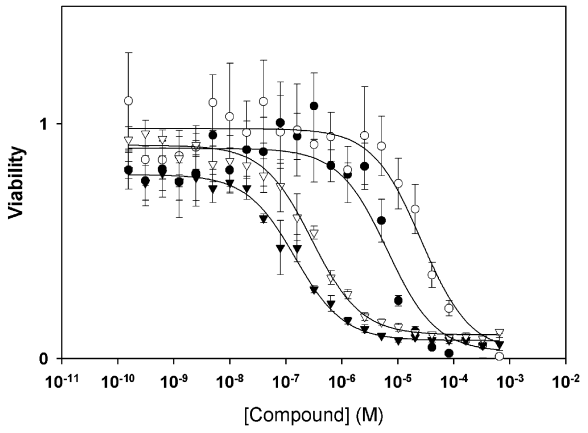

Figure 4. Effect of tetrazolium red and tetrazolium violet on *P. falciparum* cultures and CHO cells. CHO cells (circles) and *P. falciparum* cultures (inverted triangles) were grown in the presence of serial dilutions of tetrazolium red (white) or tetrazolium violet (black) and the viability of the cultures was then determined. Data points are the mean of four determinations with the standard error indicated by error bars. The IC_{50} values of individual compounds were determined using a non-linear regression analysis of the dose–response curve and IC_{50} values of 71 ± 15 μM and 338 ± 150 nM were obtained for tetrazolium red with CHO and *P. falciparum* cultures, respectively, and 15 ± 3 μM and 148 ± 45 nM were obtained for tetrazolium violet with CHO and *P. falciparum* cultures, respectively.

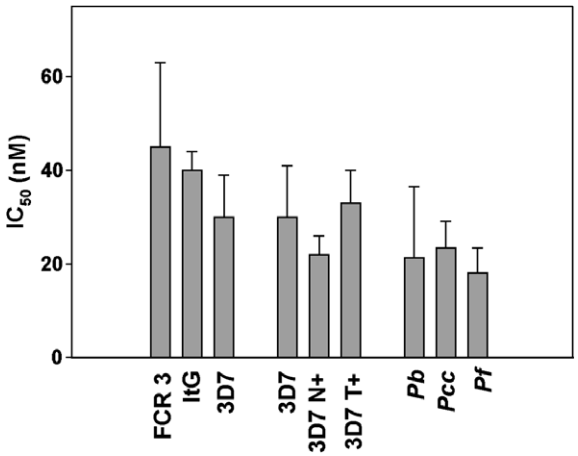

Figure 5. Activities of tetrazolium violet in human and rodent malaria cultures. Parasite viability was assayed using the SYBR-Green method.[33] Trypsin and neuraminidase treatments of human erythrocytes were as described by Lobo et al.[9] and the presence of a specific invasion phenotype was confirmed by attempting to culture parasites in erythrocytes that had been subjected to the opposite treatment. Bars represent the mean of four determinations with the standard error indicated by error bars. The IC_{50} values of individual compounds were determined using a non-linear regression analysis of the dose–response curve. The first three bars represent the results seen in three different parasite lines; the next three represent results observed for the laboratory line that had not been selected (3D7); that had been selected to grow in neuraminidase treated erythrocytes (3D7 N+); or the line in trypsin treated erythrocytes (3D7 T+). The IC_{50} values for *P. chabaudi chabaudi* (*Pcc*), *P. berghei* (*Pb*), and *P. falciparum* ItG (*Pf*) are indicated.

4. Conclusions

In summary, it would appear from the present series of compounds that most of the compounds that are active possess an aromatic group at the R^1 position, and the size of the group is not critical. Nitro modifications of active compounds are poorly tolerated, however, the presence of halogen atoms on aromatic R^2 and R^3 groups has little effect on potency. Methoxy groups are tolerated on R^2 and R^3 components, however, they are disruptive when on the R^1 component. These observations suggest that the R^1 component is interacting with a specific hydrophobic environment and the R^2 and R^3 components are less constrained. The activity of these compounds in several human and mouse *Plasmodium* cultures suggests that the compounds interact with a component of the parasite that is both essential and conserved.

5. Experimental

5.1. General

Flash column chromatography was performed on Silicycle silica gel (230–400 mesh, 60Å). Analytical thin-layer chromatography was performed on glass-backed precoated silica gel 60 F_{254} plates (Silicycle), and the compounds were visualized either by UV illumination (254 nm), or by heating after spraying with phosphomolybdic acid in ethanol. Melting points were taken on a Mel-Temp II apparatus and are uncorrected. ^1H and

^{13}C NMR spectra were recorded on Bruker Avance 300, 400, and 500 spectrometers in $CDCl_3$, $(CD_3)_2CO$, CD_3OD, or $(CD_3)_2SO$. The chemical shifts are reported in δ (ppm) relative to tetramethylsilane.[28] High-resolution ES mass spectra were recorded on a Fisons VG Quattro triple quadrupole mass spectrometer; peaks reported as *m*/*z*. Elemental analyses were performed by MHW Laboratories (Phoenix, AZ).

5.2. Materials

All chemical reagents were obtained from Sigma–Aldrich and were used without further purification. Tetrazolium red, tetrazolium violet, iodonitrotetrazolium chloride, thiazoyl blue tetrazolium bromide, neotetrazolium chloride, tetrazolium blue chloride, nitrotetrazolium blue chloride (NBT), and tetranitroblue tetrazolium chloride were purchased from Sigma–Aldrich. *tert*-Butyl hypochlorite was freshly prepared as previously described.[29]

5.3. General procedure for the formation of hydrazones by way of the condensation of aldehydes and hydrazines, as outlined in Scheme 1

The hydrazine derivative (10 mmol, usually stabilized by the addition of 10% by weight H_2O) in methanol (60 mL) was heated at reflux temperature until all of the solids were dissolved. A solution of the aldehyde (10 mmol) in methanol (25 mL) was then added in one portion, followed by a few drops of concentrated HCl. The mixture was heated at reflux temperature with stirring for 1 h and then concentrated. The crude product was extracted into ethyl acetate, the organic extract washed three times with brine, dried over $CaCl_2$, and then concentrated. The hydrazone product was purified by recrystallization from either methanol or ethyl acetate and used in the next step.

5.4. General procedure for the formation of formazans by way of the azo coupling of freshly prepared diazonium salts with hydrazones, as outlined in Scheme 1

To a solution of the aromatic amine (11 mmol) in water (25 mL) was added concentrated HCl (7.5 mL). The mixture was cooled to 0 °C using an ice–water bath. After 20 min, a solution of sodium nitrite (0.7 g, 10 mmol) in water (3 mL) was added, and the mixture stirred at 0 °C for 0.5 h. The freshly prepared diazonium salt solution was then added dropwise to a stirring solution of the hydrazone (10 mmol, prepared in Section 5.3) in pyridine (25 mL) at 0 °C. The mixture was kept at 0 °C for an additional 2 h, then extracted with ethyl acetate (150 mL). The organic extract was washed with brine (3 × 30 mL), dried over $CaCl_2$, and concentrated. Flash column chromatography on silica gel (1:3 v/v EtOAc–hexanes) of the residue gave the crude formazan which was used in the next step.

5.5. General procedure for the formation of tetrazolium salts by way of the oxidation of formazans using *tert*-butyl hypochlorite, as outlined in Scheme 1

The crude formazan (0.1 mmol, prepared in Section 5.4) was dissolved in chloroform (30 mL) and the solution was cooled to 0 °C using an ice–water bath. Freshly prepared *tert*-butyl hypochlorite[18] (0.15 mmol) was then added dropwise, the mixture stirred at 0 °C for 1 h, and then concentrated. Ether was then added and the resulting precipitate of the tetrazolium chloride product was removed by filtration and washed thoroughly with ether.

As previously noted[30] the tetrazolium salts are sensitive to light. The freshly prepared samples change color within a few hours; NMR analysis indicated the formation of the corresponding formazans in addition to other oxidation products. Thus, the tetrazolium salts were isolated and characterized with minimum exposure to light, and then stored in the dark at −20 °C until further use.

5.6. Characterization of the synthesized tetrazolium salts

5.6.1. 5-(4-Methoxyphenyl)-3-(4-nitrophenyl)-2-phenyl-3*H*-tetrazol-2-ium chloride (QT-1). Prepared using 4-nitrophenylhydrazine, 4-methoxybenzaldehyde, and aniline as starting materials to give the product; ^1H NMR (300 MHz, DMSO-d_6): δ 3.93 (s, 3H), 7.32 (d, J = 8.8 Hz, 2H), 7.74 (t, J = 7.9 Hz, 2H), 7.82–7.95 (m, 3H), 8.15 (d, J = 9.1 Hz, 2H), 8.30 (d, J = 9.0 Hz, 2H), 8.55 (d, J = 9.1 Hz, 2H); HRMS (ES) $[M-H]^-$ calcd for $C_{20}H_{15}N_5O_3Cl$: 408.0857. Found: 408.0848; HRMS (ES) $[M-Cl]^+$ calcd for $C_{20}H_{16}N_5O_3$: 374.1247. Found: 374.1250.

5.6.2. 5-(4-Bromophenyl)-3-(4-nitrophenyl)-2-phenyl-3*H*-tetrazol-2-ium chloride (QT-2). Prepared using 4-nitrophenylhydrazine, 4-bromobenzaldehyde, and aniline as starting materials to give the product; ^1H NMR (300 MHz, DMSO-d_6): δ 7.16–8.00 (m, 5H), 8.02 (d, J = 8.5 Hz, 2H), 8.24 (d, J = 5.9 Hz, 2H), 8.30 (d, J = 8.5 Hz, 2H), 8.56 (d, J = 8.9 Hz, 2H); HRMS (ES) $[M-H]^-$ calcd for $C_{19}H_{12}N_5O_2ClBr$: 455.9857. Found: 455.9848; HRMS (ES) $[M-Cl]^+$ calcd for $C_{19}H_{13}N_5O_2Br$: 422.0247. Found: 422.0243.

5.6.3. 3-(4-Nitrophenyl)-2,5-diphenyl-3*H*-tetrazol-2-ium chloride (QT-3). Prepared using 4-nitrophenylhydrazine, benzaldehyde, and aniline as starting materials to give the product; ^1H NMR (300 MHz, DMSO-d_6): δ 7.42–7.48 (m, 2H), 7.72–8.02 (m, 6H), 8.22 (d, J = 8.9 Hz, 2H), 8.36 (d, J = 6.8 Hz, 2H), 8.56 (d, J = 9.0 Hz, 2H); HRMS (ES) $[M-H]^-$ calcd for $C_{19}H_{13}N_5O_2Cl$: 378.0752. Found: 378.0735; HRMS (ES) $[M-Cl]^+$ calcd for $C_{19}H_{14}N_5O_2$: 344.1142. Found: 344.1135.

5.6.4. 5-(4-Benzyloxyphenyl)-3-(4-nitrophenyl)-2-phenyl-3*H*-tetrazol-2-ium chloride (QT-4). Prepared using 4-nitrophenylhydrazine, 4-benzyloxybenzaldehyde, and aniline as starting materials to give the product; ^1H NMR (300 MHz, DMSO-d_6): δ 5.29 (s, 2H), 7.36–7.53 (m, 8H), 7.74–7.97 (m, 4H), 8.16 (d, J = 9.0 Hz, 2H), 8.33 (d, J = 8.9 Hz, 2H), 8.56 (d, J = 9.1 Hz, 2H); HRMS (ES) $[M-H]^-$ calcd for $C_{26}H_{19}N_5O_3Cl$: 484.1190. Found: 484.1170; HRMS (ES) $[M-Cl]^+$ calcd for $C_{26}H_{20}N_5O_3$: 450.1560. Found: 450.1558.

5.6.5. 5-(4-Acetoxy-3,5-dimethoxyphenyl)-3-(4-nitrophenyl)-2-phenyl-3*H*-tetrazol-2-ium chloride (QT-5). Pre-

pared using 4-nitrophenylhydrazine, 4-acetoxy-3,5-dimethoxybenzaldehyde, and aniline as starting materials to give the product; ^{1}H NMR (300 MHz, DMSO-d_6): δ 2.30 (s, 3H), 3.90 (s, 6H), 7.40–8.00 (m, 7H), 8.20 (d, J = 8.9 Hz, 2H), 8.56 (d, J = 9.0 Hz, 2H); HRMS (ES) $[M-H]^+$ calcd for $C_{23}H_{19}N_5O_6Cl$: 496.1018. Found: 496.1027; HRMS (ES) $[M-COCH_3]^+$ calcd for $C_{21}H_{17}N_5O_5Cl$: 454.0912, found: 454.0931.

5.6.6. 5-(4-Benzyloxyphenyl)-2,3-diphenyl-3*H*-tetrazol-2-ium chloride (QT-6). Prepared using phenylhydrazine, 4-benzyloxybenzaldehyde, and aniline as starting materials to give the product; ^{1}H NMR (300 MHz, DMSO-d_6): δ 5.28 (s, 2H), 7.38–7.53 (m, 9H), 7.69–7.94 (m, 8H), 8.29 (d, J = 8.7 Hz, 2H); HRMS (ES) $[M-H]^+$ calcd for $C_{26}H_{20}N_4OCl$: 439.1320. Found: 439.1336; HRMS (ES) $[M-Cl]^+$ calcd for $C_{26}H_{21}N_4O$: 405.1709. Found: 405.1713.

5.6.7. 5-(4-Benzyloxy-3-methoxyphenyl)-2,3-diphenyl-3*H*-tetrazol-2-ium chloride (QT-7). Prepared using phenylhydrazine, 4-benzyloxy-3-methoxybenzaldehyde, and aniline as starting materials to give the product; ^{1}H NMR (300 MHz, DMSO-d_6): δ 3.91 (s, 3H), 5.30 (s, 2H), 7.39–7.58 (m, 8H), 7.70–7.94 (m, 10H); HRMS (ES) $[M-H]^+$ calcd for $C_{27}H_{22}N_4O_2Cl$: 469.1425. Found: 469.1426.

5.6.8. 5-Naphthalen-1-yl-2,3-diphenyl-3*H*-tetrazol-2-ium chloride (QT-8). Prepared using phenylhydrazine, 1-naphthaldehyde, and aniline as starting materials to give the product; ^{1}H NMR (300 MHz, DMSO-d_6): δ 7.50–8.00 (m, 11H), 8.20 (d, J = 8.9 Hz, 2H), 8.41–8.46 (m, 2H), 8.75–8.84 (m, 2H); HRMS (ES) $[M-H]^+$ calcd for $C_{23}H_{16}N_4Cl$: 383.1058. Found: 383.1061; HRMS (ES) $[M-Cl]^+$ calcd for $C_{23}H_{17}N_4$: 349.1447. Found: 349.1455.

5.6.9. 5-Biphenyl-4-yl-2,3-diphenyl-3*H*-tetrazol-2-ium chloride (QT-9). Prepared using phenylhydrazine, biphenyl-4-carboxaldehyde, and aniline as starting materials to give the product as a beige solid; ^{1}H NMR (300 MHz, DMSO-d_6): δ 7.46–7.59 (m, 4H), 7.71–8.00 (m, 11H), 8.10 (d, J = 8.1 Hz, 2H), 8.41–8.45 (m, 2H); HRMS (ES) $[M-H]^+$ calcd for $C_{25}H_{18}N_4Cl$: 409.1214. Found: 409.1222; HRMS (ES) $[M-Cl]^+$ calcd for $C_{25}H_{19}N_4$: 375.1604. Found: 375.1606.

5.6.10. 2-Biphenyl-4-yl-5-naphthalen-1-yl-3-phenyl-3*H*-tetrazol-2-ium chloride (QT-10). Prepared using phenylhydrazine, 1-naphthaldehyde, and 4-aminobiphenyl as starting materials to give the product as a white solid; ^{1}H NMR (300 MHz, DMSO-d_6): δ 7.40–7.60 (m, 4H), 7.74–8.15 (m, 14H), 8.20–8.85 (m, 3H); HRMS (ES) $[M-H]^+$ calcd for $C_{29}H_{20}N_4Cl$: 459.1371. Found: 459.1376; HRMS (ES) $[M-Cl]^+$ calcd for $C_{29}H_{21}N_4$: 425.1760. Found: 425.1761.

5.6.11. 5-Biphenyl-4-yl-3-(4-methoxyphenyl)-2-phenyl-3*H*-tetrazol-2-ium chloride (QT-11). Prepared using 4-methoxyphenylhydrazine, biphenyl-4-carboxaldehyde, and aniline as starting materials to give the product; ^{1}H NMR (300 MHz, DMSO-d_6): δ 3.87 (s, 3H), 7.20–7.29 (m, 2H), 7.48–7.59 (m, 4H), 7.74–8.00 (m, 8H), 8.09 (d, J = 8.2 Hz, 2H), 8.40 (d, J = 6.8 Hz, 2H); HRMS (ES) $[M-H]^+$ calcd for $C_{26}H_{20}N_4OCl$: 439.1320. Found: 439.1334; HRMS (ES) $[M-Cl]^+$ calcd for $C_{26}H_{21}N_4O$: 405.1709. Found: 405.1703.

5.6.12. 3-(4-Fluorophenyl)-2,5-diphenyl-3*H*-tetrazol-2-ium chloride (QT-12). Prepared using phenylhydrazine, benzaldehyde, and 4-fluoroaniline as starting materials to give the product; ^{1}H NMR (300 MHz, DMSO-d_6): δ 7.53–8.07 (m, 12H), 8.33 (d, J = 5.9 Hz, 2H); HRMS (ES) $[M-H]^+$ calcd for $C_{19}H_{13}N_4FCl$: 351.0807. Found: 351.0813; HRMS (ES) $[M-Cl]^+$ calcd for $C_{19}H_{14}N_4F$: 317.1197. Found: 317.1189.

5.6.13. 5-(4-Benzyloxyphenyl)-3-(4-fluorophenyl)-2-phenyl-3*H*-tetrazol-2-ium chloride (QT-13). Prepared using phenylhydrazine, 4-benzyloxybenzaldehyde, and 4-fluoroaniline as starting materials to give the product; ^{1}H NMR (300 MHz, DMSO-d_6): δ 5.29 (s, 2H), 7.38–7.53 (m, 8H), 7.58–7.66 (m, 2H), 7.70–7.75 (m, 1H), 7.80–7.98 (m, 5H), 8.29 (d, J = 8.4 Hz, 2H); HRMS (ES) $[M-H]^+$ calcd for $C_{26}H_{19}N_4OFCl$: 457.1225. Found: 457.1223; HRMS (ES) $[M-Cl]^+$ calcd for $C_{26}H_{20}N_4OF$: 423.1615. Found: 423.1631.

5.6.14. 5-Biphenyl-4-yl-3-(4-fluorophenyl)-2-phenyl-3*H*-tetrazol-2-ium chloride (QT-14). Prepared using phenylhydrazine, biphenyl-4-carboxaldehyde, and 4-fluoroaniline as starting materials to give the product as a beige solid; ^{1}H NMR (300 MHz, DMSO-d_6): δ 7.46–7.68 (m, 5H), 7.72–7.78 (m, 2H), 7.82–7.98 (m, 5H), 8.00–8.06 (m, 2H), 8.11 (d, J = 7.4 Hz, 2H), 8.43 (d, J = 8.2 Hz, 2H); HRMS (ES) $[M-H]^+$ calcd for $C_{25}H_{17}N_4FCl$: 427.1120. Found: 427.1134; HRMS (ES) $[M-Cl]^+$ calcd for $C_{25}H_{18}N_4F$: 393.1510. Found: 393.1520.

5.6.15. 5-Biphenyl-4-yl-3-(4-fluorophenyl)-2-(4-methoxyphenyl)-3*H*-tetrazol-2-ium chloride (QT-15). Prepared using 4-methoxyphenylhydrazine, biphenyl-4-carboxaldehyde, and 4-fluoroaniline as starting materials to give the product; ^{1}H NMR (300 MHz, DMSO-d_6): δ 3.87 (s, 3H), 7.26 (d, J = 9.1 Hz, 2H), 7.49–7.67 (m, 5H), 7.81 (d, J = 9.1 Hz, 2H), 7.85 (d, J = 6.3 Hz, 2H), 7.98–8.02 (m, 2H), 8.10 (d, J = 8.4 Hz, 2H), 8.41 (d, J = 8.4 Hz, 2H); HRMS (ES) $[M-Cl]^+$ calcd for $C_{26}H_{20}N_4OF$: 423.1615. Found: 423.1617.

5.6.16. 3-(4-Fluorophenyl)-5-naphthalen-1-yl-2-phenyl-3*H*-tetrazol-2-ium chloride (QT-16). Prepared using phenylhydrazine, 1-naphthaldehyde, and 4-fluoroaniline as starting materials to give the product; ^{1}H NMR (300 MHz, DMSO-d_6): δ 7.64–7.70 (m, 2H), 7.77–7.90 (m, 6H), 7.97–8.12 (m, 4H), 8.22 (d, J = 8.0 Hz, 1H), 8.26–8.52 (m, 2H), 8.80 (d, J = 7.9 Hz, 1H); HRMS (ES) $[M-H]^+$ calcd for $C_{23}H_{15}N_4FCl$: 401.0963. Found: 401.0972; HRMS (ES) $[M-Cl]^+$ calcd for $C_{23}H_{16}N_4F$: 367.1353. Found: 367.1346.

5.6.17. 3-(2-Fluorophenyl)-2,5-diphenyl-3*H*-tetrazol-2-ium chloride (QT-17). Prepared using phenylhydrazine, benzaldehyde, and 2-fluoroaniline as starting materials to give the product; mp 110–144 °C (dec); ^{1}H NMR (300 MHz, DMSO-d_6): δ 7.58–7.63 (m, 1H), 7.70–8.00

(m, 10H), 8.05–8.14 (m, 1H), 8.34–8.35 (m, 2H); HRMS (ES) $[M-H]^+$ calcd for $C_{19}H_{13}N_4FCl$: 351.0807. Found: 351.0814; HRMS (ES) $[M-Cl]^+$ calcd for $C_{19}H_{14}N_4F$: 317.1197. Found: 317.1190.

5.6.18. 5-(4-Benzyloxyphenyl)-3-(2-fluorophenyl)-2-phenyl-3*H*-tetrazol-2-ium chloride (QT-18). Prepared using phenylhydrazine, 4-benzyloxybenzaldehyde, and 2-fluoroaniline as starting materials to give the product; ^1H NMR (300 MHz, DMSO-d_6): δ 5.30 (s, 2H), 7.36–7.48 (m, 6H), 7.52 (d, $J = 7.6$ Hz, 2H), 7.56–7.62 (m, 1 H), 7.69–7.77 (m, 2H), 7.82–8.00 (m, 4H), 8.06–8.12 (m, 1H), 8.26–8.30 (m, 2H); HRMS (ES) $[M-H]^+$ calcd for $C_{26}H_{19}N_4OFCl$: 457.1225. Found: 457.1225; HRMS (ES) $[M-Cl]^+$ calcd for $C_{26}H_{20}N_4OF$: 423.1615. Found: 423.1606.

5.6.19. 5-Biphenyl-4-yl-3-(2-fluorophenyl)-2-phenyl-3*H*-tetrazol-2-ium chloride (QT-19). Prepared using phenylhydrazine, biphenyl-4-carboxaldehyde, and 2-fluoroaniline as starting materials to give the product; ^1H NMR (300 MHz, DMSO-d_6): δ 7.43–7.64 (m, 6H), 7.73–8.05 (m, 9H), 8.10 (d, $J = 8.2$ Hz, 2H), 8.35–8.43 (m, 1H); HRMS (ES) $[M-H]^+$ calcd for $C_{25}H_{17}N_4FCl$: 427.1120. Found: 427.1110; HRMS (ES) $[M-Cl]^+$ calcd for $C_{25}H_{18}N_4F$: 393.1510. Found: 393.1518.

5.6.20. 5-(4-Benzyloxy-3-methoxyphenyl)-3-(2-fluorophenyl)-2-phenyl-3*H*-tetrazol-2-ium chloride (QT-20). Prepared using phenylhydrazine, 4-benzyloxy-3-methoxybenzaldehyde, and 2-fluoroaniline as starting materials to give the product; ^1H NMR (300 MHz, DMSO-d_6): δ 3.92 (s, 3H), 5.31 (s, 2H), 7.39–7.52 (m, 7H), 7.54–7.62 (m, 2H), 7.68–7.80 (m, 3H), 7.86–8.05 (m, 5H); HRMS (ES) $[M-H]^+$ calcd for $C_{27}H_{21}N_4O_2FCl$: 487.1331. Found: 487.1333.

5.6.21. 3-(3-Fluorophenyl)-2,5-diphenyl-3*H*-tetrazol-2-ium chloride (QT-21). Prepared using phenylhydrazine, benzaldehyde, and 3-fluoroaniline as starting materials to give the product; ^1H NMR (300 MHz, DMSO-d_6): δ 7.73–7.89 (m, 9H), 7.99–8.07 (m, 3H), 8.31–8.36 (m, 2H); HRMS (ES) $[M-H]^+$ calcd for $C_{19}H_{13}N_4FCl$: 351.0807. Found: 351.0812; HRMS (ES) $[M-Cl]^+$ calcd for $C_{19}H_{14}N_4F$: 317.1197. Found: 317.1189.

5.6.22. 5-(4-Benzyloxyphenyl)-3-(3-fluorophenyl)-2-phenyl-3*H*-tetrazol-2-ium chloride (QT-22). Prepared using phenylhydrazine, 4-benzyloxybenzaldehyde, and 3-fluoroaniline as starting materials to give the product; ^1H NMR (300 MHz, DMSO-d_6): δ 5.28 (s, 2H), 7.37–7.65 (m, 8H), 7.72–7.94 (m, 5H), 8.00–8.19 (m, 3H), 8.27–8.37 (m, 2H); HRMS (ES) $[M-H]^+$ calcd for $C_{26}H_{19}N_4OFCl$: 457.1225. Found: 457.1225; HRMS (ES) $[M-Cl]^+$ calcd for $C_{26}H_{20}N_4OF$: 423.1615. Found: 423.1611.

5.6.23. 5-Biphenyl-4-yl-3-(3-fluorophenyl)-2-phenyl-3*H*-tetrazol-2-ium chloride (QT-23). Prepared using phenylhydrazine, biphenyl-4-carboxaldehyde, and 3-fluoroaniline as starting materials to give the product as a beige solid; ^1H NMR (300 MHz, DMSO-d_6): δ 7.44–7.81 (m, 11H), 7.93–8.01 (m, 2H), 8.34–8.55 (m, 5H); HRMS (ES) $[M-H]^+$ calcd for $C_{25}H_{17}N_4FCl$: 427.1120. Found: 427.1111; HRMS (ES) $[M-Cl]^+$ calcd for $C_{25}H_{18}N_4F$: 393.1510. Found: 393.1523.

5.6.24. 5-(4-Benzyloxy-3-methoxyphenyl)-3-(3-fluorophenyl)-2-phenyl-3*H*-tetrazol-2-ium chloride (QT-24). Prepared using phenylhydrazine, 4-benzyloxy-3-methoxybenzaldehyde, and 3-fluoroaniline as starting materials to give the product; ^1H NMR (300 MHz, DMSO-d_6): δ 3.92 (s, 3H), 5.31 (s, 2H), 7.42–7.58 (m, 7H), 7.69–8.07 (m, 10H); HRMS (ES) $[M-H]^+$ calcd for $C_{27}H_{21}N_4O_2FCl$: 487.1331. Found: 487.1309.

5.6.25. 3-(4-Chlorophenyl)-2,5-diphenyl-3*H*-tetrazol-2-ium chloride (QT-25). Prepared using phenylhydrazine, benzaldehyde, and 4-chloroaniline as starting materials to give the product as a beige solid; ^1H NMR (300 MHz, DMSO-d_6): δ 7.75–7.94 (m, 12H), 8.33–8.37 (m, 2H); HRMS (ES) $[M-H]^+$ calcd for $C_{19}H_{13}N_4Cl_2$: 367.0511. Found: 367.0521; HRMS (ES) $[M-Cl]^+$ calcd for $C_{19}H_{14}N_4Cl$: 333.0901. Found: 333.0889.

5.6.26. 5-(4-Benzyloxyphenyl)-3-(4-chlorophenyl)-2-phenyl-3*H*-tetrazol-2-ium chloride (QT-26). Prepared using phenylhydrazine, 4-benzyloxybenzaldehyde, and 4-chloroaniline as starting materials to give the product; ^1H NMR (300 MHz, DMSO-d_6): δ 5.29 (s, 2H), 7.38–7.53 (m, 8H), 7.74–7.76 (m, 2H), 7.81–7.91 (m, 6H), 8.30 (d, $J = 8.8$ Hz, 2H); HRMS (ES) $[M-H]^+$ calcd for $C_{26}H_{19}N_4OCl_2$: 473.0930. Found: 473.0920; HRMS (ES) $[M-Cl]^+$ calcd for $C_{26}H_{20}N_4OCl$: 439.1320. Found: 439.1341.

5.6.27. 5-Biphenyl-4-yl-3-(4-chlorophenyl)-2-phenyl-3*H*-tetrazol-2-ium chloride (QT-27). Prepared using phenylhydrazine, biphenyl-4-carboxaldehyde, and 4-chloroaniline as starting materials to give the product as a biege solid; ^1H NMR (300 MHz, DMSO-d_6): δ 7.48–7.51 (m, 1H), 7.57 (t, $J = 7.0$ Hz, 2H), 7.76–7.78 (m, 1H), 7.82–8.00 (m, 10H), 8.10 (d, $J = 8.3$ Hz, 2H), 8.40–8.44 (m, 2H); HRMS (ES) $[M-H]^+$ calcd for $C_{25}H_{17}N_4Cl_2$: 443.0824. Found: 443.0834; HRMS (ES) $[M-Cl]^+$ calcd for $C_{25}H_{18}N_4Cl$: 409.1214. Found: 409.1213.

5.6.28. 5-(4-Benzyloxy-3-methoxyphenyl)-3-(4-chlorophenyl)-2-phenyl-3*H*-tetrazol-2-ium chloride (QT-28). Prepared using phenylhydrazine, 4-benzyloxy-3-methoxybenzaldehyde, and 4-chloroaniline as starting materials to give the product; ^1H NMR (300 MHz, DMSO-d_6): δ 3.91 (s, 3H), 5.30 (s, 2H), 7.32–7.57 (m, 7H), 7.69–8.00 (m, 10H); HRMS (ES) $[M-H]^+$ calcd for $C_{27}H_{21}N_4O_2Cl_2$: 503.1036. Found: 503.1054.

5.6.29. 5-Biphenyl-4-yl-3-(4-chlorophenyl)-2-(4-methoxyphenyl)-3*H*-tetrazol-2-ium chloride (QT-29). Prepared using 4-methoxyphenylhydrazine, biphenyl-4-carboxaldehyde, and 4-chloroaniline as starting materials to give the product; ^1H NMR (300 MHz, DMSO-d_6): δ 3.87 (s, 3H), 7.26 (d, $J = 8.8$ Hz, 2H), 7.49 (d, $J = 9.3$ Hz, 2H), 7.56 (t, $J = 7.8$ Hz, 2H), 7.84–7.88 (m, 4H), 7.97 (d, $J = 8.9$ Hz, 2H), 8.09 (d, $J = 8.4$ Hz, 2H), 8.41 (d, $J = 8.4$ Hz, 2H), 8.67 (d, $J = 9.4$ Hz, 1H); ^{13}C NMR (75 MHz, DMSO-d_6): δ 56.1, 115.5, 117.2, 121.7,

125.1, 127.0, 127.9, 128.2, 128.4, 129.2, 130.6, 131.8, 136.2, 138.3, 138.9, 144.8, 163.0, 163.7; HRMS (ES) $[M-H]^+$ calcd for $C_{26}H_{19}N_4OCl_2$: 473.0930. Found: 473.0943; HRMS (ES) $[M-Cl]^+$ calcd for $C_{26}H_{20}N_4OCl$: 439.1320. Found: 439.1337.

5.6.30. 3-(3-Chlorophenyl)-2,5-diphenyl-3*H*-tetrazol-2-ium chloride (QT-30). Prepared using phenylhydrazine, benzaldehyde, and 3-chloroaniline as starting materials to give the product; ^{1}H NMR (300 MHz, DMSO-d_6): δ 7.73–8.12 (m, 12H), 8.34–8.36 (m, 2H); HRMS (ES) $[M-H]^+$ calcd for $C_{19}H_{13}N_4Cl_2$: 367.0511. Found: 367.0497; HRMS (ES) $[M-Cl]^+$ calcd for $C_{19}H_{14}N_4Cl$: 333.0901. Found: 333.0893.

5.6.31. 5-(4-Benzyloxyphenyl)-3-(3-chlorophenyl)-2-phenyl-3*H*-tetrazol-2-ium chloride (QT-31). Prepared using phenylhydrazine, 4-benzyloxybenzaldehyde, and 3-chloroaniline as starting materials to give the product; mp 169–171 °C; ^{1}H NMR (300 MHz, DMSO-d_6): δ 5.28 (s, 2H), 7.38–7.45 (m, 5H), 7.51 (d, J = 7.1 Hz, 2H), 7.72–8.08 (m, 9H), 8.32 (d, J = 8.9 Hz, 2H); ^{13}C NMR (100 MHz, CD_3OD): δ 70.0, 115.1, 116.0, 124.5, 125.8, 125.9, 127.3, 127.9, 128.3, 129.3, 130.4, 130.7, 131.7, 133.2, 134.0, 134.2, 135.8, 136.4, 152.4, 163.2; HRMS (ES) $[M-H]^+$ calcd for $C_{26}H_{19}N_4OCl_2$: 473.0930. Found: 473.0948; HRMS (ES) $[M-Cl]^+$ calcd for $C_{26}H_{20}N_4OCl$: 439.1320. Found: 439.1313.

5.6.32. 5-Biphenyl-4-yl-3-(3-chlorophenyl)-2-phenyl-3*H*-tetrazol-2-ium chloride (QT-32). Prepared using phenylhydrazine, biphenyl-4-carboxaldehyde, and 3-chloroaniline as starting materials to give the product; ^{1}H NMR (300 MHz, DMSO-d_6): δ 7.46–7.59 (m, 4H), 7.76–8.19 (m, 12H), 8.34–8.44 (m, 2H); HRMS (ES) $[M-H]^+$ calcd for $C_{25}H_{17}N_4Cl_2$: 443.0824. Found: 443.0832; HRMS (ES) $[M-Cl]^+$ calcd for $C_{25}H_{18}N_4Cl$: 409.1214. Found: 409.1211.

5.6.33. 5-(4-Benzyloxy-3-methoxyphenyl)-3-(3-chlorophenyl)-2-phenyl-3*H*-tetrazol-2-ium chloride (QT-33). Prepared using phenylhydrazine, 4-benzyloxy-3-methoxybenzaldehyde, and 3-chloroaniline as starting materials to give the product; ^{1}H NMR (300 MHz, DMSO-d_6): δ 3.40 (s, 3H), 5.31 (s, 2H), 7.38–7.52 (m, 8H), 7.58 (s, 1H), 7.70–7.78 (m, 3H), 7.86–7.96 (m, 4H), 8.00–8.07 (m, 1H); HRMS (ES) $[M-H]^+$ calcd for $C_{27}H_{21}N_4O_2Cl_2$: 503.1036. Found: 503.1027; HRMS (ES) $[M-Cl]^+$ calcd for $C_{27}H_{22}N_4O_2Cl$: 469.1425. Found: 469.1417.

5.6.34. 2-(4-Methoxyphenyl)-3,5-diphenyl-3*H*-tetrazol-2-ium chloride (QT-34). Prepared using phenylhydrazine, benzaldehyde, and 4-methoxyaniline as starting materials to give the product; ^{1}H NMR (300 MHz, DMSO-d_6): δ 3.86 (s, 3H), 7.21–7.26 (m, 2H), 7.77–7.96 (m, 10H), 8.32–8.34 (m, 2H); HRMS (ES) $[M-H]^+$ calcd for $C_{20}H_{16}N_4OCl$: 363.1007. Found: 363.1023; HRMS (ES) $[M-Cl]^+$ calcd for $C_{20}H_{17}N_4O$: 329.1396. Found: 329.1409.

5.6.35. 5-(4-Benzyloxyphenyl)-2-(4-methoxyphenyl)-3-phenyl-3*H*-tetrazol-2-ium chloride (QT-35). Prepared using phenylhydrazine, 4-benzyloxybenzaldehyde, and 4-methoxyaniline as starting materials to give the product; ^{1}H NMR (300 MHz, DMSO-d_6): δ 3.86 (s, 3H), 5.28 (s, 2H), 7.23–7.25 (m, 2H), 7.37–7.64 (m, 8H), 7.72–7.91 (m, 6H), 8.26–8.38 (m, 2H); HRMS (ES) $[M-H]^+$ calcd for $C_{27}H_{22}N_4O_2Cl$: 469.1425. Found: 469.1418; HRMS (ES) $[M-Cl]^+$ calcd for $C_{27}H_{23}N_4O_2$: 435.1815. Found: 435.1817.

5.6.36. 3-(4-Nitrophenyl)-2,5-diphenyl-3*H*-tetrazol-2-ium chloride (QT-36). Prepared using phenylhydrazine, benzaldehyde, and 4-nitroaniline as starting materials to give the product; ^{1}H NMR (300 MHz, DMSO-d_6): δ 7.75–8.01 (m, 7H), 8.10–8.30 (m, 2H), 8.35–8.41 (m, 2H), 8.50–8.61 (m, 2H), 8.69–8.82 (m, 1H); HRMS (ES) $[M-H]^+$ calcd for $C_{19}H_{13}N_5O_2Cl$: 378.0752. Found: 378.0753; HRMS (ES) $[M-Cl]^+$ calcd for $C_{19}H_{14}N_5O_2$: 344.1142. Found: 344.1155.

5.6.37. 5-(4-Nitrophenyl)-2,3-diphenyl-3*H*-tetrazol-2-ium chloride (QT-37). Prepared using phenylhydrazine, 4-nitrobenzaldehyde, and aniline as starting materials to give the product; ^{1}H NMR (300 MHz, DMSO-d_6): δ 7.74–7.77 (m, 3H), 7.82–7.97 (m, 7H), 8.58–8.63 (m, 4H); HRMS (ES) $[M-H]^+$ calcd for $C_{19}H_{13}N_5O_2Cl$: 378.0752. Found: 378.0765; HRMS (ES) $[M-Cl]^+$ calcd for $C_{19}H_{14}N_5O_2$: 344.1142. Found: 344.1140.

5.6.38. 5-(4-Benzyloxyphenyl)-3-(3-chlorophenyl)-2-(4-methoxyphenyl)-3*H*-tetrazol-2-ium chloride (QT-38). Prepared using 4-methoxyphenylhydrazine, 4-benzyloxybenzaldehyde, and 3-chloroaniline as starting materials to give the product; ^{1}H NMR (300 MHz, DMSO-d_6): δ 3.86 (s, 3H), 5.28 (s, 2H), 7.20–7.29 (m, 2H), 7.38–7.55 (m, 7H), 7.74–8.07 (m, 5H), 8.25–8.30 (m, 2H), 8.60–8.65 (m, 1H); HRMS (ES) $[M-H]^+$ calcd for $C_{27}H_{21}N_4O_2Cl_2$: 503.1036. Found: 503.1049; HRMS (ES) $[M-Cl]^+$ calcd for $C_{27}H_{22}N_4O_2Cl$: 469.1425. Found: 469.1438.

5.6.39. 2-(4-Benzyloxyphenyl)-3,5-diphenyl-3*H*-tetrazol-2-ium chloride (QT-39). Prepared using phenylhydrazine, benzaldehyde, and 4-benzyloxyaniline as starting materials to give the product as a beige solid; mp 90–120 °C (dec); ^{1}H NMR (300 MHz, DMSO-d_6): δ 5.22 (s, 2H), 7.29–7.48 (m, 7H), 7.71–7.98 (m, 10H), 8.32–8.34 (m, 2H); HRMS (ES) $[M-H]^+$ calcd for $C_{26}H_{20}N_4OCl$: 439.1320. Found: 439.1334; HRMS (ES) $[M-Cl]^+$ calcd for $C_{26}H_{21}N_4O$: 405.1709. Found: 405.1706.

5.6.40. 2,5-Bis-(4-benzyloxyphenyl)-3-phenyl-3*H*-tetrazol-2-ium chloride (QT-40). Prepared using phenylhydrazine, 4-benzyloxybenzaldehyde, and 4-benzyloxyaniline as starting materials to give the product; ^{1}H NMR (300 MHz, DMSO-d_6): δ 5.20 (s, 2H), 5.28 (s, 2H), 7.28–7.53 (m, 15H), 7.73–7.92 (m, 6H), 8.26–8.29 (m, 2H); HRMS (ES) $[M-H]^+$ calcd for $C_{33}H_{26}N_4O_2Cl$: 545.1738. Found: 545.1727; HRMS (ES) $[M-Cl]^+$ calcd for $C_{33}H_{27}N_4O_2$: 511.2128. Found: 511.2145.

5.6.41. 2-(4-Benzyloxyphenyl)-5-(3-chlorophenyl)-3-phenyl-3*H*-tetrazol-2-ium chloride (QT-41). Prepared using

phenylhydrazine, 3-chlorobenzaldehyde, and 4-benzyloxyaniline as starting materials to give the product; ^{1}H NMR (300 MHz, DMSO-d_6): δ 5.22 (s, 2H), 7.29–7.48 (m, 7H), 7.71–8.02 (m, 9H), 8.28–8.35 (m, 2H); HRMS (ES) $[M-H]^+$ calcd for $C_{26}H_{19}N_4OCl_2$: 473.0930. Found: 473.0929; HRMS (ES) $[M-Cl]^+$ calcd for $C_{26}H_{20}N_4OCl$: 439.1320. Found: 439.1329.

5.6.42. 2-(4-Benzyloxyphenyl)-5-biphenyl-4-yl-3-phenyl-3*H*-tetrazol-2-ium chloride (QT-42). Prepared using phenylhydrazine, biphenyl-4-carboxaldehyde, and 4-benzyloxyaniline as starting materials to give the product as a beige solid; ^{1}H NMR (300 MHz, DMSO-d_6): δ 5.22 (s, 2 H), 7.31–7.59 (m, 10H), 7.75–7.96 (m, 9H), 8.10 (d, J = 8.4 Hz, 2H), 8.39–8.43 (m, 2H); HRMS (ES) $[M-H]^+$ calcd for $C_{32}H_{24}N_4OCl$: 515.1633. Found: 515.1609; HRMS (ES) $[M-Cl]^+$ calcd for $C_{32}H_{25}N_4O$: 481.2022. Found: 481.2016.

5.6.43. 2-(4-Benzyloxyphenyl)-3-(3-chlorophenyl)-5-phenyl-3*H*-tetrazol-2-ium chloride (QT-43). Prepared using 3-chlorophenylhydrazine, benzaldehyde, and 4-benzyloxyaniline as starting materials to give the product; mp 95–125 °C (dec); ^{1}H NMR (300 MHz, DMSO-d_6): δ 5.44 (s, 2H), 7.36–7.60 (m, 10H), 7.79–7.95 (m, 5H), 8.18–8.33 (m, 2H), 8.69–8.71 (m, 1H); HRMS (ES) $[M-H]^+$ calcd for $C_{26}H_{19}N_4OCl_2$: 473.0930. Found: 473.0937; HRMS (ES) $[M-Cl]^+$ calcd for $C_{26}H_{20}N_4OCl$: 439.1320. Found: 439.1341.

5.6.44. 5-(4-Benzyloxyphenyl)-3-(3-chlorophenyl)-2-phenyl-3*H*-tetrazol-2-ium chloride (QT-44). Prepared using 3-chlorophenylhydrazine, 4-benzyloxybenzaldehyde, and aniline as starting materials to give the product; ^{1}H NMR (300 MHz, DMSO-d_6): δ 5.29 (s, 2H), 7.35–7.53 (m, 8H), 7.72–8.08 (m, 8H), 8.27–8.36 (m, 2H); HRMS (ES) $[M-H]^+$ calcd for $C_{26}H_{19}N_4OCl_2$: 473.0930. Found: 473.0934; HRMS (ES) $[M-Cl]^+$ calcd for $C_{26}H_{20}N_4OCl$: 439.1320. Found: 439.1325.

5.6.45. 5-(3-Chlorophenyl)-2,3-diphenyl-3*H*-tetrazol-2-ium chloride (QT-45). Prepared using phenylhydrazine, 3-chlorobenzaldehyde, and aniline as starting materials to give the product; mp 104–128 °C (dec); ^{1}H NMR (300 MHz, DMSO-d_6): δ 7.70–7.77 (m, 3H), 7.79–7.87 (m, 4H), 7.90–8.06 (m, 5H), 8.31–8.34 (m, 1H), 8.36–8.37 (m, 1H); HRMS (ES) $[M-H]^+$ calcd for $C_{19}H_{13}N_4Cl_2$: 367.0511. Found: 367.0497; HRMS (ES) $[M-Cl]^+$ calcd for $C_{19}H_{14}N_4Cl$: 333.0901. Found: 333.0915.

5.6.46. 2,3-Bis-(3-chlorophenyl)-5-phenyl-3*H*-tetrazol-2-ium chloride (QT-46). Prepared using 3-chlorophenylhydrazine, benzaldehyde, and 3-chloroaniline as starting materials to give the product; ^{1}H NMR (300 MHz, DMSO-d_6): δ 7.76–7.85 (m, 6H), 7.92–8.08 (m, 4H), 8.17 (s, 1H), 8.34–8.45 (m, 2H); HRMS (ES) $[M-H]^+$ calcd for $C_{19}H_{12}N_4Cl_3$: 401.0127. Found: 401.0143; HRMS (ES) $[M-Cl]^+$ calcd for $C_{19}H_{13}N_4Cl_2$: 367.0511. Found: 367.0522.

5.6.47. 5-(4-Benzyloxyphenyl)-2,3-bis-(3-chlorophenyl)-3*H*-tetrazol-2-ium chloride (QT-47). Prepared using 3-chlorophenylhydrazine, 4-benzyloxybenzaldehyde, and 3-chloroaniline as starting materials to give the product as a beige solid; ^{1}H NMR (300 MHz, DMSO-d_6): δ 5.29 (s, 2H), 7.42–7.62 (m, 9H), 7.75–7.80 (m, 1H), 7.88–8.09 (m, 4H), 8.12 (s, 1H), 8.28–8.31 (m, 2H); HRMS (ES) $[M-H]^+$ calcd for $C_{26}H_{18}N_4OCl_3$: 507.0546. Found: 507.0553; HRMS (ES) $[M-Cl]^+$ calcd for $C_{26}H_{19}N_4OCl_2$: 473.0935. Found: 473.0936.

5.6.48. 3-(3-Bromophenyl)-2,5-diphenyl-3*H*-tetrazol-2-ium chloride (QT-48). Prepared using phenylhydrazine, benzaldehyde, and 3-bromoaniline as starting materials to give the product; ^{1}H NMR (300 MHz, DMSO-d_6): δ 7.67–8.08 (m, 11H), 8.20–8.25 (m, 1H), 8.38–8.46 (m, 2H); HRMS (ES) $[M-H]^+$ calcd for $C_{19}H_{13}N_4ClBr$: 411.0006. Found: 411.0020; HRMS (ES) $[M-Cl]^+$ calcd for $C_{19}H_{14}N_4Br$: 377.0396. Found: 377.0392.

5.6.49. 5-(4-Benzyloxyphenyl)-3-(3-bromophenyl)-2-phenyl-3*H*-tetrazol-2-ium chloride (QT-49). Prepared using phenylhydrazine, 4-benzyloxybenzaldehyde, and 3-bromoaniline as starting materials to give the product; ^{1}H NMR (300 MHz, DMSO-d_6): δ 5.29 (s, 2H), 7.36–7.53 (m, 8H), 7.66–8.14 (m, 8H), 8.29–8.33 (m, 2H); HRMS (ES) $[M-H]^+$ calcd for $C_{26}H_{19}N_4OClBr$: 517.0430. Found: 517.0458; HRMS (ES) $[M-Cl]^+$ calcd for $C_{26}H_{20}N_4OBr$: 483.0820. Found: 483.0810.

5.6.50. 5-Hexyl-2,3-diphenyl-3*H*-tetrazol-2-ium bromide (QT-50). Prepared using phenylhydrazine, heptaldehyde, and aniline as starting materials to give the product as a white solid; ^{1}H NMR (300 MHz, CD_3OD): δ 0.97 (t, J = 6.9 Hz, 3H), 1.44–1.46 (m, 4H), 1.61–1.66 (m, 2H), 2.06 (m, 2H), 3.33 (t, J = 7.6 Hz, 2H), 7.65–7.71 (m, 4H), 7.78–7.83 (m, 6H); ^{13}C NMR (400 MHz, CD_3OD): δ 13.0, 22.1, 25.4, 26.6, 28.3, 31.2, 125.9, 130.2, 133.3, 133.8, 168.5; HRMS (ES) $[M-Br]^+$ calcd for $C_{19}H_{23}N_4$: 307.1917. Found: 307.1923.

5.6.51. 5-Cyclohexyl-2,3-diphenyl-3*H*-tetrazol-2-ium chloride (QT-51). Prepared using phenylhydrazine, cyclohexanecarboxaldehyde, and aniline as starting materials to give the product; ^{1}H NMR (300 MHz, DMSO-d_6): δ 1.46 (t, J = 2.1 Hz, 1H), 1.54–1.66 (m, 2H), 1.84–1.92 (m, 3H), 1.96–2.00 (m, 2H), 2.36–2.40 (m, 2H), 3.35–3.50 (m, 1H), 7.65–7.86 (m, 10H); HRMS (ES) $[M-H]^+$ calcd for $C_{19}H_{20}N_4Cl$: 339.1376. Found: 339.1361; HRMS (ES) $[M-Cl]^+$ calcd for $C_{19}H_{21}N_4$: 305.1766. Found: 305.1755.

5.6.52. 2,3-Diphenyl-5-(4-undecyloxyphenyl)-3*H*-tetrazol-2-ium chloride (QT-52). Prepared using phenylhydrazine, 4-undecyloxybenzaldehyde, and aniline as starting materials to give the product; ^{1}H NMR (300 MHz, DMSO-d_6): δ 0.86 (t, J = 6.3 Hz, 3H), 1.26–1.46 (m, 16H), 1.75–1.80 (m, 2H), 4.11–4.24 (m, 2H), 7.28 (d, J = 8.7 Hz, 2H), 7.66–7.93 (m, 10H), 8.26 (d, J = 8.7 Hz, 2H); HRMS (ES) $[M-H]^+$ calcd for $C_{30}H_{36}N_4OCl$: 503.2577. Found: 503.2582; HRMS (ES) $[M-Cl]^+$ calcd for $C_{30}H_{37}N_4O$: 469.2967. Found: 469.2965.

5.6.53. 2,3-Diphenyl-5-(3-undecyloxyphenyl)-3*H*-tetrazol-2-ium chloride (QT-53). Prepared using phenylhydr-

azine, 3-undecyloxybenzaldehyde, and aniline as starting materials to give the product; ^{1}H NMR (300 MHz, DMSO-d_6): δ 0.75–0.90 (m, 3H), 1.10–1.50 (m, 16H), 1.60–1.80 (m, 2H), 4.00–4.25 (m, 2H), 7.30–7.40 (m, 1H), 7.60–7.90 (m, 6H), 7.95–8.25 (m, 6H), 8.75–8.90 (m, 1H); HRMS (ES) $[M-H]^+$ calcd for $C_{30}H_{36}N_4OCl$: 503.2577. Found: 503.2579; HRMS (ES) $[M-Cl]^+$ calcd for $C_{30}H_{37}N_4O$: 469.2967. Found: 469.2965.

5.6.54. 5-Isopropyl-2,3-diphenyl-3*H*-tetrazol-2-ium bromide (QT-54). Prepared using phenylhydrazine, isobutyraldehyde, and aniline as starting materials to give the product; ^{1}H NMR (300 MHz, CD_3OD): δ 1.65 (d, J = 7.0 Hz, 6H), 3.66–3.70 (m, 1H), 7.66–7.83 (m, 10H); ^{13}C NMR (75 MHz, CD_3OD): δ 19.5, 26.8, 125.8, 130.2, 133.4, 133.8, 172.7; HRMS (ES) $[M-Br]^+$ calcd for $C_{16}H_{17}N_4$: 265.1447. Found: 265.1456.

5.7. Assays for the inhibition of the reduction of tetrazolium salts

Assays were performed in a 96-well plate. Nitrotetrazolium blue chloride (NBT) was added to a final concentration as indicated on the x-axis (see Fig. 2) and glutathione was added to a final concentration of 7 mM. β-Cyclodextrin, either unsulfated or having an average of one sulfate group per glucose residue,[10] was added to a final concentration ranging from 0 to 167 μM. All solutions were prepared in 50 mM Tris buffer, pH 9.0.[19] Assays were performed by adding 50 μL of the NBT solution to a microwell followed by 50 μL of the β-cyclodextrin solution, allowing the plate to incubate for 5 min, and then adding 50 μL of the glutathione solution. Ten minutes after the addition of the glutathione solution the plates were read at 650 nm in a ThermoMax microplate reader (Molecular Devices, Sunnyvale, CA.). To determine the effect of SITS (4-acetamido-4′-isothiocyanato-2,2′-stilbenedisulfonic acid disodium salt, Molecular Probes, Inc.) and DIDS (4,4′-diisothiocyanatostilbene-2,2′-disulfonic acid disodium salt, Sigma) on the reduction of NBT serial dilutions of the compounds were prepared in 50 μL of Tris buffer and then 50 μL of 30 μM NBT was added to every well, followed by 50 μL of 21 mM glutathione. After 10 min, the absorbance at 650 nm was determined as above.

5.8. Determination of anti-*Plasmodium* activity

P. falciparum cultures were grown in O+ blood obtained by venipuncture of volunteers. Cultures of the laboratory line ItG were maintained by the method of Trager and Jensen[31] using RPMI-1640 supplemented with 10% human serum (a kind gift obtained under ethical consent from the Chemo Day Care Department of the Princess Margaret Hospital, Toronto, Canada) and 50 μM hypoxanthine (RPMI-A). The effects of the test compounds on the viability of *P. falciparum* cultures were determined using a Lactate Dehydrogenase (LDH) enzyme assay specific for the enzyme found in *Plasmodium falciparum* (pLDH).[19,32] Briefly, compounds to be tested were dissolved in DMSO to afford a solution having a concentration of 10 mg/mL. Twofold serial dilutions were then produced in 50 μL of RPMI-A in a 96-well plate and then 50 μL of parasite culture (2% hematocrit, 2% parasitemia) was added to each well and the plates were then incubated at 37 °C in 95% N_2, 3% CO_2, and 2% O_2 for 72 h. The contents of the wells were then re-suspended using a multi-channel pipettor and a 15-μL sample was removed from each well and was added to 100 μL of pLDH enzyme assay mixture.[19] After 1 h the absorbance of the wells at 650 nm was determined using a ThermoMax microplate reader (Molecular Devices, Sunnyvale, CA). The IC_{50} values of individual compounds were determined using a non-linear regression analysis of the data[33] using the computer program SigmaPlot (Jandel Scientific). The IC_{50} values represent means ± standard error calculated from four independent determinations. To verify if the poor viability of the cultures was related to inhibited merozoite invasion, samples were taken from treated wells and the presence of extracellular merozoites was confirmed by microscopy.

Assays comparing the activity of the compounds in human and rodent malaria cultures were performed in a similar fashion, however, parasite viability was assayed using the SYBR-Green method.[33] Rodent malaria samples were obtained by cardiac puncture of infected mice and the erythrocytes were then cultured for two days in compound diluted in RPMI-1640. Trypsin and neuraminidase treatment of human erythrocytes was performed as described by Lobo et al.,[9] and the presence of a specific invasion phenotype was confirmed by attempting to culture parasites in erythrocytes that had been subjected to the opposite treatment.

5.9. Mammalian strains and culture

CHO cells (ATCC, Manassas, VA) were grown in RPMI-1640 supplemented with 10% fetal calf serum (Sigma, St. Louis, MO), 25 mM Hepes, and gentimicin (RPMI-10). Cells were seeded in 96-well plates and grown to 50% confluency in 100 μL of RPMI-10 per well prior to the addition of either DMSO alone, or a 10 mg/mL solution of a tetrazolium compound in DMSO. Compound gradients were prepared by adding 90 μL of RPMI-10 mixed with 10 μL of compound solution to the first well in the series, mixing, transferring 100 μL to next well, and repeating until the next-to-last well was reached. After 48 h, the viability of the cells was determined by discarding the media in the wells and adding 100 μL of 10 mg/mL of 3-[4,5-dimethylthiazol-2-yl]-2,5-diphenyltetrazolium bromide (MTT, Sigma, St. Louis, MO) in RPMI-10, incubating the plates for a further hour, and then removing the media and adding 100 μL of DMSO and reading the absorbance at 650 nm.[21] The IC_{50} values of individual compounds were determined using a non-linear regression analysis of the dose-response curve using the computer program SigmaPlot (Jandel Scientific).

Acknowledgments

The authors gratefully acknowledge the generous support of the Bill and Melinda Gates Foundation, and

the award of a CIHR Proof of Principle Grant PPP-62029 to IC.

References and notes

1. Breman, J. G.; Egan, A.; Keusch, G. T. *Am. J. Trop. Med. Hyg.* **2001**, *64*, iv–vii, See also http://rbm.who.int/wmr2005/ for the World Health Organization World Malaria Report 2005.
2. Wkly. Epidemiol. Rec. **1997**, *72*, 277.
3. White, N. J.; Nosten, F.; Looareesuwan, S.; Watkins, W. M.; Marsh, K.; Snow, R. W.; Kokwaro, G.; Ouma, J.; Hien, T. T.; Molyneux, M. E.; Taylor, T. E.; Newbold C. I.; Ruebush, T. K., 2nd; Danis, M.; Greenwood, B. M.; Anderson, R. M.; Olliaro, P. *Lancet* **1999**, *353*, 1965.
4. Kisilevsky, R.; Crandall, I.; Szarek, W. A.; Bhat, S.; Tan, C.; Boudreau, L.; Kain, K. C. *Antimicrob. Agents Chemother.* **2002**, *46*, 2619.
5. Pasvol, G. *Trends Parasitol.* **2003**, *19*, 430.
6. Pasvol, G.; Wainscoat, J. S.; Weatherall, D. J. *Nature* **1982**, *297*, 64.
7. Barnwell, J. W.; Galinski, M. R. In *Malaria: Parasite Biology, Pathogenesis, and Protection*; Sherman, I. W., Ed.; ASM Press: Washington, DC, 1998; pp 93–123.
8. Oh, S. S.; Chishti, A. H. *Curr. Top. Microbiol. Immunol.* **2005**, *295*, 203.
9. Lobo, C. A.; de Frazao, K.; Rodriguez, M.; Reid, M.; Zalis, M.; Lustigman, S. *Infect. Immun.* **2004**, *72*, 5886.
10. Crandall, I. E.; Szarek, W. A.; Vlahakis, J. Z.; Xu, Y.; Vohra, R.; Sui, J.; Kisilevsky, R. *Biochem. Pharmacol.* **2007**, *73*, 632.
11. Xiao, L.; Yang, C.; Patterson, P. S.; Udhayakumar, V.; Lal, A. A. *Infect. Immun.* **1996**, *64*, 1373.
12. Popov, M.; Li, J.; Reithmeier, R. A. *Biochem. J.* **1999**, *339*, 269.
13. Salhany, J. M.; Schopfer, L. M. *Biochemistry* **1996**, *35*, 251.
14. Salhany, J. M.; Schopfer, L. M.; Kay, M. M.; Gamble, D. N.; Lawrence, C. *Proc. Natl. Acad. Sci. U.S.A.* **1995**, *92*, 11844.
15. Hamzé, A.; Rubi, E.; Arnal, P.; Boisbrun, M.; Carcel, C.; Salom-Roig, X.; Maynadier, M.; Wein, S.; Vial, H.; Calas, M. *J. Med. Chem.* **2005**, *48*, 3639; Wengelnik, K.; Vidal, V.; Ancelin, M. L.; Cathiard, A-M.; Morgat, J. L.; Kocken, C. H.; Calas, M.; Herrera, S.; Thomas, A. W.; Vial, H. J. *Science* **2002**, *295*, 1311.
16. Katritzky, A. R.; Belyakov, S. A.; Cheng, D.; Durst, H. D. *Synthesis* **1995**, 577.
17. Ashley, J. N.; Davis, B. M.; Nineham, A. W.; Slack, R. *J. Chem. Soc.* **1953**, 3881.
18. Benson, F. R.; Otten, E. A.; Schachat, R. E. *J. Am. Chem. Soc.* **1954**, *76*, 1695.
19. Prudhomme, J. G.; Sherman, I. W. *J. Immunol. Methods* **1999**, *229*, 169.
20. Pimplikar, S. W.; Reithmeier, R. A. *J. Biol. Chem.* **1986**, *261*, 9770.
21. Campling, B. G.; Pym, J.; Galbraith, P. R.; Cole, S. P. *Leukocyte Res.* **1988**, *12*, 823.
22. Perkins, M. E.; Holt, E. H. *Mol. Biochem. Parasitol.* **1988**, *27*, 23.
23. Clark, D. L.; Su, S.; Davidson, E. A. *Glycoconj. J.* **1997**, *14*, 473.
24. Higuti, T.; Arakaki, R.; Kotera, Y.; Takigawa, M.; Tani, I.; Shibuya, M. *Biochim. Biophys. Acta* **1983**, *725*, 1.
25. Goel, V. K.; Li, X.; Chen, H.; Liu, S. C.; Chishti, A. H.; Oh, S. S. *Proc. Natl. Acad. Sci. U.S.A.* **2003**, *100*, 5164.
26. Kariuki, M. M.; Li, X.; Yamodo, I.; Chishti, A. H.; Oh, S. S. *Biochem. Biophys. Res. Commun.* **2005**, *338*, 1690.
27. Casey, J. R.; Reithmeier, R. A. *Biochemistry* **1993**, *32*, 1172.
28. Gottlieb, H. E.; Kotlyar, V.; Nudelman, A. *J. Org. Chem.* **1997**, *62*, 7512.
29. Mintz, M. J.; Walling, C. *Org. Synth.* **1969**, *49*, 9.
30. Nineham, A. W. *Chem. Rev.* **1955**, *55*, 355.
31. Trager, W.; Jensen, J. B. *Science* **1976**, *193*, 673.
32. Makler, M. T.; Ries, J. M.; Williams, J. A.; Bancroft, J. E.; Piper, R. C.; Gibbins, B. L.; Hinrichs, D. J. *Am. J. Trop. Med. Hyg.* **1993**, *48*, 739.
33. Smilkstein, M.; Sriwilaijaroen, N.; Kelly, J. X.; Wilairat, P.; Riscoe, M. *Antimicrob. Agents Chemother.* **2004**, *48*, 1803.